Journal of Visualized Experiments

Phospho Flow Cytometry with Fluorescent Cell Barcoding for Single Cell Signaling Analysis and Biomarker Discovery

--Manuscript Draft--

Article Type:	Invited Methods Article - JoVE Produced Video
Manuscript Number:	JoVE58386R2
Full Title:	Phospho Flow Cytometry with Fluorescent Cell Barcoding for Single Cell Signaling Analysis and Biomarker Discovery
Keywords:	Biomarker; cell signaling; Chronic lymphocytic leukemia (CLL); Fluorescent cell barcoding (FCB); Phospho flow; Phospho-proteins; Single cell profiling
Corresponding Author:	Sigrid S Skånland, PhD University of Oslo Oslo, Oslo NORWAY
Corresponding Author's Institution:	University of Oslo
Corresponding Author E-Mail:	sigrid.skanland@ncmm.uio.no
Order of Authors:	Sigrid S Skånland, PhD
Additional Information:	
Question	**Response**
Please indicate whether this article will be Standard Access or Open Access.	Standard Access (US$2,400)
Please indicate the **city, state/province, and country** where this article will be **filmed**. Please do not use abbreviations.	Centre for Molecular Medicine Norway, Forskningsparken, Gaustadalleen 21, 0349 Oslo, Norway

Powered by Editorial Manager® and ProduXion Manager® from Aries Systems Corporation

Manuscript Click here to download Manuscript 58386_R2.docx

TITLE:

Phospho Flow Cytometry with Fluorescent Cell Barcoding for Single Cell Signaling Analysis and Biomarker Discovery

AUTHORS AND AFFILIATIONS:
Sigrid S. Skånland[1, 2]

[1]Centre for Molecular Medicine Norway (NCMM), Nordic EMBL Partnership, University of Oslo, Oslo, Norway
[2]K. G. Jebsen Centre for B cell malignancies and K. G. Jebsen Centre for Cancer Immunotherapy, University of Oslo, Oslo, Norway

sigrid.skanland@ncmm.uio.no

KEYWORDS:
Biomarker, Cell Signaling, Chronic Lymphocytic Leukemia (CLL), Fluorescent Cell Barcoding (FCB), Phospho Flow Cytometry, Phospho-Proteins, Single Cell Profiling

SUMMARY:
Here, a protocol for medium- to high-throughput analysis of protein phosphorylation events at the cellular level is presented. Phospho flow cytometry is a powerful approach to characterize signaling aberrations, identify and validate biomarkers, and assess pharmacodynamics.

ABSTRACT:
Aberrant cell signaling plays a central role in cancer development and progression. Most novel targeted therapies are indeed directed at proteins and protein functions, and cell signaling aberrations may therefore serve as biomarkers to indicate personalized treatment options. As opposed to DNA and RNA analyses, changes in protein activity can more efficiently evaluate the mechanisms underlying drug sensitivity and resistance. Phospho flow cytometry is a powerful technique that measures protein phosphorylation events at the cellular level, an important feature that distinguishes this method from other antibody-based approaches. The method allows for simultaneous analysis of multiple signaling proteins. In combination with fluorescent cell barcoding, larger medium- to high-throughput data-sets can be acquired by standard cytometer hardware in short time. Phospho flow cytometry has applications both in studies of basic biology and in clinical research, including signaling analysis, biomarker discovery and assessment of pharmacodynamics. Here, a detailed experimental protocol is provided for phospho flow analysis of purified peripheral blood mononuclear cells, using chronic lymphocytic leukemia cells as an example.

INTRODUCTION:
Phospho flow cytometry is used to analyze protein phosphorylation levels at single-cell resolution. The overall goal of the method is to map cellular signaling patterns under specified conditions. By exploiting the multiparameter capacity of flow cytometry, several signaling pathways can be analyzed simultaneously in different subsets of a heterogeneous cell

population such as peripheral blood. These traits offer advantages over other antibody-based technologies such as immunohistochemistry, enzyme-linked immunosorbent assay (ELISA), protein array, and reverse phase protein array (RPPA)[1]. Phospho flow cytometry can be combined with fluorescent cell barcoding (FCB), which means that individual cell samples are labeled with unique signatures of fluorescent dyes so that they can be mixed together, stained and analyzed as a single sample[2]. This reduces the antibody consumption, increases the data robustness through the combination of control and treated samples, and enhances the speed of acquisition. The combined FCB population can then be divided into smaller samples and stained with up to 35 distinct phospho-specific antibodies, depending on the amount of starting material. Large profiling experiments can, thereby, be run with standard cytometer hardware. Phospho flow cytometry has been applied to profile signaling pathways in patient samples from several hematological cancers including chronic lymphocytic leukemia (CLL)[3-5], acute myeloid leukemia (AML)[6] and non-Hodgkin lymphomas[7]. Phospho flow cytometry is thus a powerful approach to characterize signaling aberrations, identify and validate biomarkers, and assess pharmacodynamics.

Here, the optimized protocol for analysis of CLL patient samples by phospho flow cytometry is provided (**Figure 1A**). Examples of basal signaling characterization, anti-IgM/B cell receptor stimulation and drug perturbation are shown. A detailed description of an FCB matrix is provided. The protocol can easily be adapted to other suspension cell types.

PROTOCOL:

Blood samples were received following written informed consent from all donors. The study was approved by the Regional Committee for Medical and Health Research Ethics of South-East Norway and the research on human blood was carried out in accordance with the Declaration of Helsinki[8].

Note: Steps 1-3 should be performed under sterile conditions in a tissue culture hood.

1. Isolation of Peripheral Blood Mononuclear Cells (PBMCs) from CLL Patient Blood Samples

CAUTION: Human blood should be handled according to regulations for Biosafety Level 2.

1.1. Dilute the blood 1:1 with phosphate-buffered saline (PBS: 136.9 mM NaCl, 2.7 mM KCl, 10.1 mM Na_2HPO_4 x $2H_2O$, 1.8 mM KH_2PO_4, pH 7.4) and transfer to 50 mL tubes (30 mL/tube).

1.2. Carefully layer 10 mL of a density gradient medium (*e.g.*, Lymphoprep) to the bottom of the tube using a 10 mL pipette.

1.3. Centrifuge at 800 x g for 20 min at 4 °C. The PBMCs are now visible on top of the density gradient medium layer.

1.4. Use a Pasteur pipette to transfer the cells into two new 50 mL tubes. Wash twice with PBS (fill up the tubes).

1.5. Centrifuge at 350 x g for 15 min. Discard the supernatant and resuspend in 3 mL of PBS.

1.6. Count the cells using a preferred method.

Note: Steps 1.7 to 3.2 are optional. It is possible to proceed directly to step 3.3.

1.7. Centrifuge the cells at 350 x g for 5 min. Discard the supernatant.

1.8. Resuspend the cells in fetal bovine serum (FBS) supplemented with 10% dimethyl sulfoxide (DMSO) and freeze down in suitable aliquots using cryo tubes.

Note: DMSO is toxic to the cells. Work fast once the cells are mixed with FBS/DMSO. Cells can be stored long term in liquid nitrogen.

2. Thawing of Cells

2.1. Quickly thaw the cells in a 37 °C water bath.

Note: DMSO is toxic to the cells. Work fast to limit the exposure to DMSO.

2.2. Wash the cells once with 10 mL of cold Roswell Park Memorial Institute medium (RPMI 1640 with supplemental GlutaMAX, see **Table of Materials**).

2.3. Centrifuge at 300 x g for 5 min. Discard the supernatant.

2.4. Resuspend the cells in RPMI 1640 medium supplemented with sodium pyruvate, MEM non-essential amino acids and penicillin/streptomycin (added at 1x dilution according to instructions) and 10% FBS. Transfer the cells to a small cell culture flask and leave in an incubator at 5% CO_2, 37 °C for 1 hour to allow the cells to calibrate.

3. Preparation of Cells

3.1. Count the viable cells using a preferred method.

3.2. Transfer the cells to a 50 mL tube and centrifuge at 300 x g for 5 min. Discard the supernatant.

3.3. Resuspend the cells in RPMI 1640 medium (step 2.2) supplemented with 1% FBS to no more than 50 x 10^6 cells/mL.

3.4. Transfer the required amount of cell suspension to wells in a 96 well V-bottom plate.

Note: Number of wells corresponds to the number of conditions to be tested. Samples for a stimulation time-course are drawn from a single well. Calculate 50 µL sample per time-point + 50 µL of dead volume. Save samples for compensation controls (one unstained sample + one sample per barcoding dye).

3.5. Transfer the 96 well plate to a pre-heated 37 °C water bath. Rest the cells for 10 min.

4. Stimulation and Fixation of Cells

Note: Perform steps 4-8 on the lab bench (*i.e.,* not sterile).

CAUTION: The main ingredient of Fix Buffer I is paraformaldehyde, which is toxic (inhalation and skin contact). Handle with care.

4.1. Prepare a 96 well V-bottom plate with 60 µL of Fix Buffer I per well per sample. Leave in the 37 °C water bath.

Note: Cells: Fix buffer should be 1:1. In order to allow for evaporation at 37 °C, the Fix buffer is initially in abundance.

4.2. Optionally, treat the cells with drugs before stimulation.

4.3. Transfer a 50 µL control sample to the fix plate. Mix by pipetting up and down.

4.4. Optionally, start the stimulation time-course by adding 10 µg/mL anti-IgM to the cells. Mix by pipetting up and down.

4.5. Transfer a 50 µL sample to the fix plate at each time-point. Mix by pipetting up and down.

Note: Anti-IgM induced signaling is usually initiated early (minutes).

4.6. Leave the fix plate at 37 °C for 10 min after the last sample has been added.

5. Fluorescent Cell Barcoding (FCB)

Note: See **Table 1** for a list of barcoding reagents.

5.1. Wash the fixed cells 3x with PBS (fill up the wells).

5.2. Centrifuge at 500 x g for 5 min. Discard the supernatant.

5.3. Prepare a 96 well V-bottom plate with barcoding reagents. Pipet 5 µL of each barcoding reagent per well in the number of combinations required to stain all samples following the

staining matrix, *e.g.,* in **Figure 1B**. Each sample will have a unique combination of different barcoding concentrations.

5.4. Resuspend the cells in 190 µL of PBS and transfer to the barcoding plate. Mix thoroughly.

Note: Stain one compensation sample with the highest final concentration used for each barcoding reagent and save one unstained sample.

5.5. Leave the cells for 20 min at room temperature, in the dark.

5.6. Wash the stained cells 2x with flow wash (PBS, 1% FBS, 0.09% sodium azide) (fill up the wells).

5.7. Centrifuge at 500 x g for 5 min. Discard the supernatant.

5.8. Add 190 µL of flow wash to the cells and combine the barcoded samples in one 15 mL tube. Transfer each compensation control to a separate 1.7 mL tube.

5.9. Centrifuge at 500 x g for 5 min. Discard the supernatant.

6. Cell Permeabilization for Intracellular Antigen Staining

CAUTION: The main ingredient of Perm Buffer III is methanol which is toxic (inhalation and skin contact) and flammable. Handle with care.

6.1. Transfer 2 mL of Perm Buffer III to a 15 mL tube. Leave at -20 °C so it is ice-cold upon use.

Note: The Perm Buffer can be left at -20 °C from the start of the experiment.

6.2. Add 1.5 mL of ice-cold Perm Buffer to the barcoded cell population (in a 15 mL tube) and 100 µL to each compensation control (in 1.7 mL tubes) drop-wise while vortexing to avoid that the cells clump together.

6.3. Transfer the cells directly to -80 °C. Leave for a minimum of 30 min.

Note: It is natural to pause the experiment at this point. Cells in Perm Buffer can be stored long term at -80 °C.

7. Antibody Staining

Note: See **Table of Materials** for a list of reported phospho-specific antibodies.

7.1. Transfer the cells from -80 °C to a box of ice.

7.2. Wash 3x with flow wash.

Note: It is important to add flow wash in excess to see the cell pellet, *e.g.,* add 3 mL of flow wash to the barcoded cell population and 1 mL to each compensation control.

7.3. Centrifuge at 500 x g for 5 min at 4 °C. Discard the supernatant.

7.4. Resuspend the barcoded cell population in a volume of flow wash, which allows 25 µL of cell suspension per phospho-antibody stain. Resuspend the compensation controls in 200 µL of flow wash.

7.5. Prepare antibodies for staining in a 96 well V-bottom plate. The final volume will be 50 µL/well. Per well, add phospho-specific antibody diluted in flow wash to a final volume of 10 µL, surface marker diluted in flow wash to a final volume of 15 µL, and 25 µL of cell suspension.

Note: Antibody dilutions should be titrated prior to the experiment. Include isotype control.

7.6. Leave the cells for 30 min at room temperature, in the dark.

7.7. Wash the stained cells 2x with flow wash (fill up the wells).

7.8. Centrifuge at 500 x g for 5 min. Discard the supernatant.

7.9. Resuspend the cells in 150 µL of flow wash.

8. Preparation of Compensation Controls

8.1. Prepare compensation controls for the antibody-conjugated fluorochromes in parallel with the antibody staining. Use compensation beads according to the vendor's instructions.

9. Flow Cytometry Analysis

Note: The experiment can be run on a flow cytometer with a High Throughput Sampler (HTS).

9.1. Optimize the photomultiplier tube (PMT) voltage with the unstained control.

9.2. Run compensation controls and calculate the compensation matrix.

9.3. Run samples. The event rate should be in accordance with the instrument specifications.

10. Gating Strategy and Data Analysis

10.1. Import the FCS files from the experiment to a flow cytometry analysis software like FlowJo or Cytobank (https://cellmass.cytobank.org).

10.2. Gating strategy

10.2.1. Select lymphocytes by plotting SSC-A *versus* FSC-A in a density dot plot.

10.2.2. Display the lymphocytes and select the singlets by plotting SSC-A *versus* FSC -W.

10.2.3. Display the single cells and gate the cell type by plotting SSC-A *versus* the surface marker.

10.2.4. Display the cell type population in a Pacific Blue *versus* SSC-A density plot and select the different FCB populations based on their Pacific Blue staining intensity (see **Figure 1A**).

10.2.5. Plot the phospho antibody channel against the FCB channel, or as a heatmap (see **Figure 1A**) to display the phosphorylation events.

10.3. Calculate phospho-signals using the inverse hyperbolic sine (arcsinh) of the MFI (median fluorescent intensity) of phospho-signal *versus* isotype control (basal phosphorylation levels, see **Figure 1D**), or of stimulated *versus* unstimulated cell populations (see **Figure 1E**).

REPRESENTATIVE RESULTS:

The main steps of the phospho flow cytometry protocol are illustrated in **Figure 1A**. In the presented example, CLL cells were stained with the barcoding reagent Pacific Blue at four dilutions. Three-dimensional barcoding can be performed by combining three barcoding dyes, as illustrated in **Figure 1B**. The individual samples are then deconvoluted by subsequent gating on each barcoding reagent *versus* SSC-A (**Figure 1C**). Detailed information about the barcoding reagents are listed in **Table 1**.

Following the procedure described here, phospho-protein levels were characterized in B cells from CLL patients and normal controls under various conditions[3]. Both basal and stimulation-induced phosphorylation levels of 20 signaling molecules downstream of the B cell receptor (BCR) were analyzed (see **Table of Materials** for a list of reported phospho-specific antibodies). Basal phospho-protein levels were mapped in 22 CLL patient samples relative to the mean of normal controls. This analysis showed that STAT3 (pY705) is significantly upregulated in CLL cells (**Figure 1D**). Constitutive activation of STAT3 has been reported in other hematological malignancies and is associated with resistance to apoptosis[9].

In order to identify signaling aberrations induced through the BCR pathway, cells were stimulated with anti-IgM for up to 30 min. It has been shown that CLL cells from patients with IgVH unmutated status (UM-CLL) display increased sensitivity towards anti-IgM stimulation[10]. This was indeed observed for the majority of the analyzed proteins, but the effect was statistically significant only for AKT (pS473) (**Figure 1E**, UM-CLL *versus* M-CLL and Normal). To test if the aberrant AKT (pS473) signal could be reversed CLL cells were exposed to the PI3Kδ inhibitor idelalisib, which is used in the clinic to treat CLL patients[11]. As shown in **Figure 1F**, AKT

308 (pS473) levels were significantly reduced upon idelalisib treatment in a concentration-
309 dependent manner, demonstrating that kinase inhibitors can be applied to normalize aberrant
310 signaling in CLL cells.
311
312 These results show that phospho flow cytometry in combination with FCB is a powerful
313 approach to perform signaling analysis studies, identify potential biomarkers, and assess
314 pharmacodynamics.
315
316 **FIGURE AND TABLE LEGENDS:**
317
318 **Figure 1. Work flow and examples of applied phospho flow cytometry analysis.**
319
320 (**A**) The main steps of the phospho flow procedure are illustrated. Cells are first stimulated,
321 then fixed and subjected to FCB before they can be combined in one tube for permeabilization
322 and subsequent antibody staining. The cells are run on a flow cytometer and the cell
323 populations are deconvoluted by gating during the data analysis. The results can be visualized
324 as histograms or heatmaps, as shown. (**B**) Example of a three-dimensional FCB staining matrix
325 using Alexa Fluor 488 (three dilutions), Pacific Blue (four dilutions) and Pacific Orange (three
326 dilutions). This matrix will allow combination of up to 36 samples. (**C**) The FCB cell population
327 can be deconvoluted by gating on each FCB channel *versus* SSC-A. Combination of the gates in
328 the analysis software generates the correct populations for analysis. (**D**) Unstimulated B cells
329 from healthy donors (n = 25) and CLL patients (n = 22) were subjected to analysis by phospho
330 flow following the procedure in (**A**). The basal fluorescence intensity signals were calculated
331 relative to IgGκ isotype control as arcsinh ratio. The signals in CLL B cells were then normalized
332 to the signals in B cells from normal controls. $^{**}p < 0.01$, calculated by an unpaired two-sample
333 t-test. UM-CLL: IgVH unmutated CLL, M-CLL: IgVH mutated CLL. Symbols of the same color
334 represent patient samples which grouped together in a hierarchical agglomerative cluster
335 based on levels of 20 phospho-proteins[3]. (**E**) B cells from normal controls (n = 10, mean + SEM)
336 or CLL patients (n = 11 [M-CLL] and n = 8 [UM-CLL], mean + SEM) were stimulated with anti-IgM
337 for the indicated time-course and subjected to phospho flow analysis. The fluorescence
338 intensity signals were measured relative to unstimulated samples and shown as arcsinh ratio.
339 $^{**}p < 0.01$ (Normal vs UM-CLL) and $^{***}p < 0.001$ (M-CLL vs UM-CLL), calculated by multiple
340 comparison testing with Holm-Sidak's correction. UM-CLL: IgVH unmutated CLL, M-CLL: IgVH
341 mutated CLL. (**F**) CLL cells were incubated with DMSO or idelalisib as indicated for 20 min
342 before anti-IgM stimulation for 3 min. The cells were then processed following the phospho
343 flow protocol. $^{*}p < 0.05$, $^{**}p < 0.01$, $^{****}p < 0.0001$, calculated by multiple comparison testing
344 with Holm-Sidak's correction. UM-CLL: IgVH unmutated CLL, M-CLL: IgVH mutated CLL. See (**D**)
345 for explanation of symbol color. (**D-F**) are modified from[3].
346
347 **Table 1.** Barcoding reagents.
348
349 **DISCUSSION:**
350 Phospho flow cytometry is a powerful technique to measure protein phosphorylation levels in
351 single cells. Since the method relies on staining with antibodies, phospho flow cytometry is

352 limited by antibody availability. Furthermore, in order to obtain reliable results, all antibodies
353 should be titrated and verified before use. A detailed protocol for titration of phospho-specific
354 antibodies has been described elsewhere[12]. During panel design, consideration of the signal-to-
355 noise ratio is critical. In the presented example, all phospho-antibodies were conjugated to
356 Alexa Fluor 647. This fluorophore often provides the optimal differential between samples with
357 low *versus* high levels of phospho-protein. Furthermore, by using only one color for the
358 phospho-proteins the other channels will be left free for FCB and surface marker staining. This
359 panel design reduces spillover into the phospho channel. By having all phospho-antibodies
360 conjugated to the same fluorophore, the data analysis will also be simplified.
361
362 In the presented protocol, all antibody stainings were performed after fixation and
363 permeabilization of the cells. However, it is important to keep in mind that surface marker
364 staining can be adversely affected by the fixation and permeabilization steps due to
365 denaturation of the surface antigen or increased nonspecific staining[13]. The user should
366 therefore test the reactivity of the antibodies on a case to case basis. Resources on compatible
367 clones may also be helpful, such as the overview of different fixation/permeabilization
368 procedures and their compatibility with various antibodies at
369 https://www.cytobank.org/facselect/.
370
371 Protein phosphorylation or de-phosphorylation is a transient modification that occurs in
372 response to both extrinsic and intrinsic cues. When comparing phosphorylation patterns, it is
373 therefore crucial that the experiments are carried out under similar conditions. When studying
374 signaling in primary cells from blood, factors that could impact the result include time elapsed
375 after drawing the blood, storage conditions and for how long the isolated cells are rested
376 before initiation of the experiment. When comparing signaling patterns in cryo preserved cells
377 and freshly isolated cells from blood, only very minor significant differences could be observed
378 (Skånland, unpublished). However, it is still advisable to use cryo preserved normal cells as a
379 control when studying biobanked patient samples, for example. The optimal conditions for
380 performing the phospho flow cytometry experiments and the impact of external factors should
381 be tested by the individual user.
382
383 Here, a protocol is presented for phospho flow analysis of suspension cells. The protocol can be
384 adapted to other cell types, but it is a prerequisite that the cells are in suspension as single cells
385 for the analysis by flow cytometry. The procedure to achieve this must be delicate to preserve,
386 and not affect, phosphorylation patterns. Examples exist where adherent cells are detached
387 from the culturing dish by cold trypsination[12,14], or are rather grown on microspheres[15]. When it
388 comes to phospho flow cytometry on solid tissue, one report exists on lung tumors where
389 single cells were obtained by passing the cells through a tube with a cell strainer[16]. Recently,
390 phospho flow cytometry was combined with a novel approach termed Disaggregation for
391 Intracellular Signaling in Single Epithelial Cells from Tissue (DISSECT) in order to study phospho-
392 proteins in epithelial tissues[17] and colorectal cancer[18].
393
394 The FCB is a critical step in the protocol since deconvolution of the samples at the end of the
395 experiment relies on distinct FCB populations. In order to obtain this, the cells need to be

396 homogeneously stained. It is therefore important to prepare a barcoding plate that the cells
397 can be added to. Adding the reagents to the cells will result in uneven staining and mixed
398 populations that cannot be deconvoluted by gating. It is highly recommended to run a test of
399 the barcoding dilutions before the experiment is performed as the staining intensity is cell-type
400 dependent.
401
402 Additional antibody-based techniques such as protein array and reverse phase protein array
403 (RPPA) can be applied for quantification of phospho-protein levels in a medium to high-
404 throughput manner. However, some qualities of phospho flow cytometry distinguish this
405 method from the others. An important advantage of phospho flow cytometry is that it allows
406 for single cell profiling. By including surface markers for different cellular subsets, inter-cellular
407 heterogeneity can be detected. Combination with FCB furthermore allows for analysis of
408 several conditions in the same experimental run. These features make phospho flow cytometry
409 an attractive method for future applications in biomarker discovery and precision medicine[19].
410
411 **ACKNOWLEDGMENTS:**
412 This work was conducted in the lab of Professor Kjetil Taskén, and was supported by the
413 Norwegian Cancer Society and Stiftelsen Kristian Gerhard Jebsen. Johannes Landskron and
414 Marianne Enger are acknowledged for critical reading of the manuscript.
415
416 **DISCLOSURES:**
417 The author has nothing to disclose.
418
419 **REFERENCES:**
420 1. Lu, Y. *et al.* Using reverse-phase protein arrays as pharmacodynamic assays for
421 functional proteomics, biomarker discovery, and drug development in cancer. *Seminars in*
422 *Oncology.* **43** (4), 476-483 (2016).
423 2. Krutzik, P.O. & Nolan, G.P. Fluorescent cell barcoding in flow cytometry allows high-
424 throughput drug screening and signaling profiling. *Nature Methods.* **3** (5), 361-368 (2006).
425 3. Myhrvold, I.K. *et al.* Single cell profiling of phospho-protein levels in chronic lymphocytic
426 leukemia. *Oncotarget.* **9** (10), 9273-9284 (2018).
427 4. Parente-Ribes, A. *et al.* Spleen tyrosine kinase inhibitors reduce CD40L-induced
428 proliferation of chronic lymphocytic leukemia cells but not normal B cells. *Haematologica.* **101**
429 (2), e59-e62 (2016).
430 5. Blix, E.S. *et al.* Phospho-specific flow cytometry identifies aberrant signaling in indolent
431 B-cell lymphoma. *BMC Cancer.* **12** 478 (2012).
432 6. Irish, J.M. *et al.* Single cell profiling of potentiated phospho-protein networks in cancer
433 cells. *Cell.* **118** (2), 217-228 (2004).
434 7. Myklebust, J.H. *et al.* Distinct patterns of B-cell receptor signaling in non-Hodgkin
435 lymphomas identified by single-cell profiling. *Blood.* **129** (6), 759-770 (2017).
436 8. World Medical Association Declaration of Helsinki: ethical principles for medical
437 research involving human subjects. *THE JOURNAL OF THE AMERICAN MEDICAL ASSOCIATION.*
438 **310** (20), 2191-2194 (2013).

439 9. Siveen, K.S. *et al.* Targeting the STAT3 signaling pathway in cancer: role of synthetic and
440 natural inhibitors. *Biochimica et Biophysica Acta.* **1845** (2), 136-154 (2014).
441 10. Fabbri, G. & Dalla-Favera, R. The molecular pathogenesis of chronic lymphocytic
442 leukaemia. *Nature Reviews Cancer.* **16** (3), 145-162 (2016).
443 11. Arnason, J.E. & Brown, J.R. Targeting B Cell Signaling in Chronic Lymphocytic Leukemia.
444 *Current Oncology Reports.* **19** (9), 61 (2017).
445 12. Landskron, J. & Tasken, K. Phosphoprotein Detection by High-Throughput Flow
446 Cytometry. *Methods in Molecular Biology.* **1355** 275-290 (2016).
447 13. Krutzik, P.O., Clutter, M.R., & Nolan, G.P. Coordinate analysis of murine immune cell
448 surface markers and intracellular phosphoproteins by flow cytometry. *Journal of Immunology.*
449 **175** (4), 2357-2365 (2005).
450 14. Pollheimer, J. *et al.* Interleukin-33 drives a proinflammatory endothelial activation that
451 selectively targets nonquiescent cells. *Arteriosclerosis, Thrombosis, and Vascular Biology.* **33** (2),
452 e47-e55 (2013).
453 15. Ertsås, H.C., Nolan, G.P., LaBarge, M.A., & Lorens, J.B. Microsphere cytometry to
454 interrogate microenvironment-dependent cell signaling. *Integrative biology: quantitative*
455 *biosciences from nano to macro.* **9** (2), 123-134 (2017).
456 16. Lin, C.C. *et al.* Single cell phospho-specific flow cytometry can detect dynamic changes of
457 phospho-Stat1 level in lung cancer cells. *Cytometry A.* **77** (11), 1008-1019 (2010).
458 17. Simmons, A.J. *et al.* Cytometry-based single-cell analysis of intact epithelial signaling
459 reveals MAPK activation divergent from TNF-alpha-induced apoptosis *in vivo*. *Molecular*
460 *Systems Biology.* **11** (10), 835 (2015).
461 18. Simmons, A.J. *et al.* Impaired coordination between signaling pathways is revealed in
462 human colorectal cancer using single-cell mass cytometry of archival tissue blocks. *Science*
463 *Signaling.* **9** (449), rs11 (2016).
464 19. Friedman, A.A., Letai, A., Fisher, D.E., & Flaherty, K.T. Precision medicine for cancer with
465 next-generation functional diagnostics. *Nature Reviews Cancer.* **15** (12), 747-756 (2015).
466
467

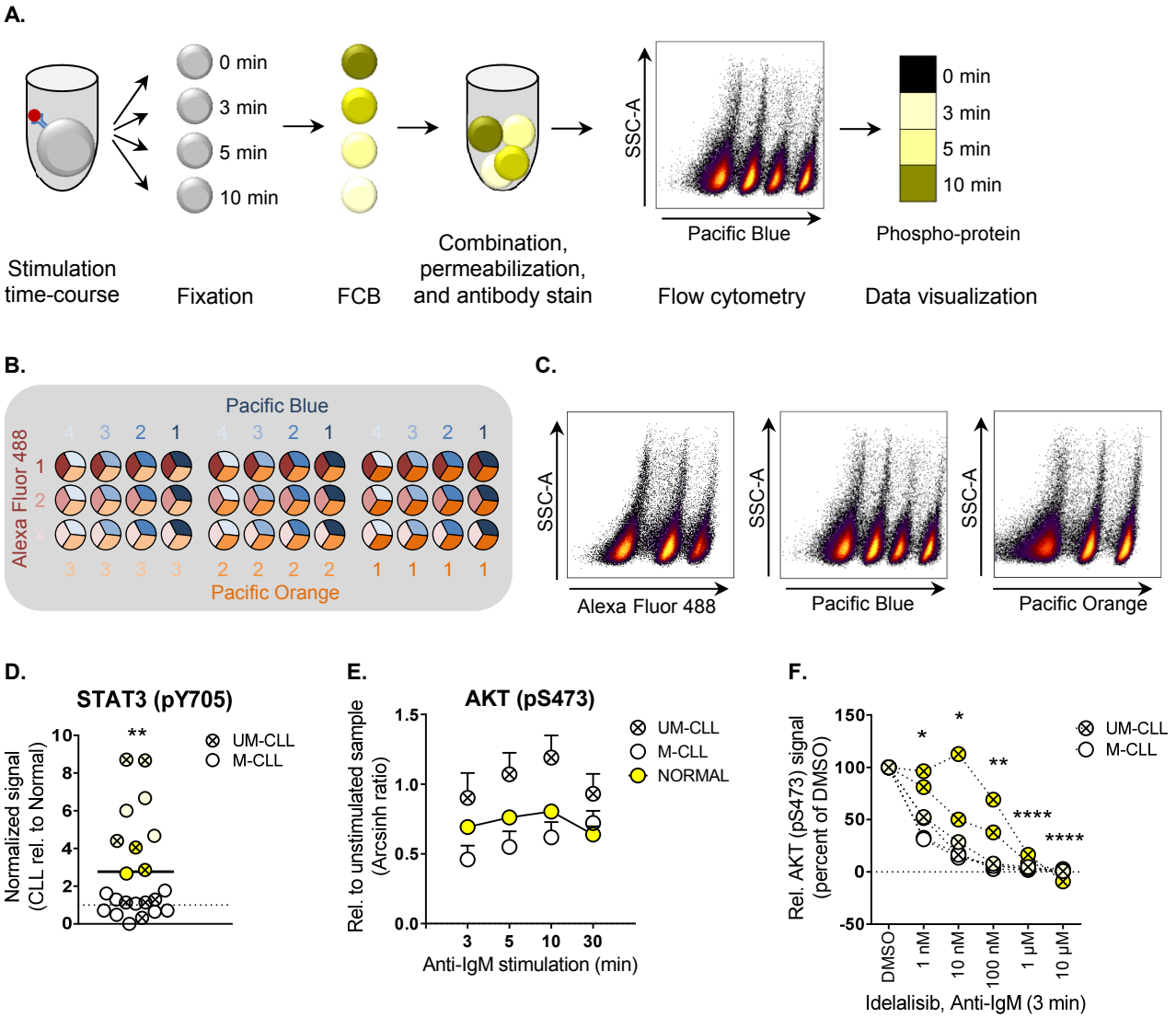
A.
0 min
3 min
5 min
10 min
SSC-A
Pacific Blue
0 min
3 min
5 min
10 min
Stimulation time-course
Fixation
FCB
Combination, permeabilization, and antibody stain
Flow cytometry
Phospho-protein
Data visualization
B.
Pacific Blue
Alexa Fluor 488
Pacific Orange
C.
SSC-A
Alexa Fluor 488
Pacific Blue
Pacific Orange
D.
STAT3 (pY705)
Normalized signal (CLL rel. to Normal)
UM-CLL
M-CLL
E.
AKT (pS473)
Rel. to unstimulated sample (Arcsinh ratio)
UM-CLL
M-CLL
NORMAL
Anti-IgM stimulation (min)
F.
Rel. AKT (pS473) signal (percent of DMSO)
UM-CLL
M-CLL
DMSO
1 nM
10 nM
100 nM
1 µM
10 µM
Idelalisib, Anti-IgM (3 min)

Figure 1

Click here to access/download
Video or Animated Figure
FIGURE 1.emf

Table

Click here to download Table Table 1 - FCB.xlsx

		Serial dilute as follows (starting with the stock solution)				
Barcoding reagent	Stock concentration	#1	#2	#3	#4	unstained
Alexa Fluor 488	10 mg/mL	1:500	1:5			x
Pacific Blue	10 mg/mL	1:2500	1:4	1:4	1:10	
Pacific Orange	2 mg/mL	1:50	1:12	1:24		

Click here to download Table of Materials JoVE_Materials.xls

Name of Material/ Equipment	Company	Catalog Number	Comments/Description
RPMI 1640 GlutaMAX	ThermoFisher Scientific	61870-010	Cell culture medium
Fetal bovine serum	ThermoFisher Scientific	10270169	Additive to cell culture medium
Sodium pyruvate	ThermoFisher Scientific	11360-039	Additive to cell culture medium
MEM non-essential amino acids	ThermoFisher Scientific	11140-035	Additive to cell culture medium
Lymphoprep	Alere Technologies AS	1114547	Density gradient medium
Anti-IgM	Southern Biotech	2022-01	For stimulation of the B cell receptor
BD Phosflow Fix Buffer I	BD	557870	Fixation buffer
BD Phosflow Perm Buffer III	BD	558050	Permeabilization buffer
Alexa Fluor 488 5-TFP	ThermoFisher Scientific	A30005	Barcoding reagent
Pacific Blue Succinimidyl Ester	ThermoFisher Scientific	P10163	Barcoding reagent
Pacific Orange Succinimidyl Ester, Triethylammonium Salt	ThermoFisher Scientific	P30253	Barcoding reagent
Compensation beads	*Defined by user*		Correct species reactivity
Falcon tubes	*Defined by user*		
Eppendorf tubes	*Defined by user*		
96 well V-bottom plates	*Defined by user*		Compatible with the flow cytometer
Centrifuges	*Defined by user*		For Eppendorf tubes, Falcon tubes and plates
Water bath	*Defined by user*		Temperature regulated
Flow cytometer	*Defined by user*		With High Throughput Sampler (HTS)

Click here to download Table of Materials JoVE_Materials - Antibodies.xlsx

Antigen	Vendor*	Clone	Cat. No.	Reference
AKT (pS473)	CST	D9E	4075	(Myhrvold et al., 2018) (Parente-Ribes et al., 2016) (Skånland et al., 2014) (Kalland et al., 2014)
ATF-2 (pT71)	SCBT	F-1	sc-8398	(Skånland et al., 2014) (Pollheimer et al., 2013)
BLNK (pY84)	BD	J117-1278	558443	(Myhrvold et al., 2018) (Parente-Ribes et al., 2016) (Kalland et al., 2014) (Myklebust et al., 2017)
Btk (pY223)/Itk (pY180)	BD	N35-86	564846	(Myklebust et al., 2017)
Btk (pY551)	BD	24a/BTK (Y551)	558129	(Kalland et al., 2014)
Btk (pY551)/Itk (pY511)	BD	24a/BTK (Y551)	558134	(Myhrvold et al., 2018) (Parente-Ribes et al., 2016)
CD3ζ (pY142)	BD	K25-407.69	558489	(Skånland et al., 2014)
Histone H3 (pS10)	CST	D2C8	9716	(Myhrvold et al., 2018)
IκBα	CST	L35A5	5743	(Myklebust et al., 2017)
LAT (pY171)	BD	I58-1169	558518	(Skånland et al., 2014)
Lck (pY505)	BD	4/LCK-Y505	558577	(Myhrvold et al., 2018)
MEK1 (pS298)	BD	J114-64	560043	(Myhrvold et al., 2018) (Skånland et al., 2014)
NF-κB p65 (pS529)	BD	K10-895.12.50	558422	(Myhrvold et al., 2018) (Skånland et al., 2014) (Kalland et al., 2014) (Pollheimer et al., 2013)
NF-κB p65 (pS536)	CST	93H1	4887	(Myhrvold et al., 2018) (Skånland et al., 2014) (Kalland et al., 2014)
p38 MAPK (pT180/Y182)	CST	28B10	4552	(Myhrvold et al., 2018) (Skånland et al., 2014) (Pollheimer et al., 2013)
p44/42 MAPK (pT202/Y204)	CST	E10	4375	(Myhrvold et al., 2018) (Parente-Ribes et al., 2016) (Skånland et al., 2014) (Kalland et al., 2014) (Pollheimer et al., 2013)
p53 (pS15)	CST	16G8	NN	(Irish et al., 2007)
p53 (pS20)	CST	Polyclonal	NN	(Irish et al., 2007)
p53 (pS37)	CST	Polyclonal	NN	(Irish et al., 2007)
p53 (pS46)	CST	Polyclonal	NN	(Irish et al., 2007)
p53 (pS392)	CST	Polyclonal	NN	(Irish et al., 2007)
PLCγ2 (pY759)	BD	K86-689.37	558498	(Myhrvold et al., 2018) (Myklebust et al., 2017)
Rb (pS807/pS811)	BD	J112-906	558590	(Myhrvold et al., 2018) (Pollheimer et al., 2013)
S6-Ribos. Prot. (pS235/236)	CST	D57.2.2E	4851	(Myhrvold et al., 2018)
SAPK/JNK (pT183/Y185)	CST	G9	9257	(Myhrvold et al., 2018) (Pollheimer et al., 2013)
SLP76 (pY128)	BD	J141-668.36.58	558438	(Skånland et al., 2014)
STAT1 (pY701)	BD	4a	612597	(Myhrvold et al., 2018) (Myklebust et al., 2017)
STAT3 (pY705)	BD	4/P-STAT3	557815	(Myhrvold et al., 2018)
STAT4 (pY693)	Zymed/TFS	Polyclonal	71-7900	(Uzel et al., 2001)
STAT5 (pY694)	BD	47/Stat5(pY694)	612599	(Myhrvold et al., 2018) (Skånland et al., 2014) (Myklebust et al., 2017)
STAT6 (pY641)	BD	18/P-Stat6	612601	(Myhrvold et al., 2018)
SYK (pY525/Y526)	CST	C87C1	12081	(Myhrvold et al., 2018) (Parente-Ribes et al., 2016)
ZAP70/SYK (pY319/Y352)	BD	17A/P-ZAP70	557817	(Skånland et al., 2014) (Kalland et al., 2014) (Myklebust et al., 2017)

*BD, Beckton Dickinson Pharmingen; CST, Cell Signaling Technologies; SCBT, Santa Cruz Biotechnology; TFS, ThermoFisher Scientific

Uzel et al., 2001, Detection of intracellular phosphorylated STAT-4 by flow cytometry, Clin Immunol, 100(3): 270-6
Irish et al., 2007, Flt3 Y591 duplication and Bcl-2 overexpression…, Blood, 109(6):2589-96
Kalland et al., 2012, Modulation of proximal signaling in normal and transformed…, Exp Cell Res, 318(14):1611-9
Pollheimer et al., 2013, Interleukin-33 drives a proinflammatory endothelial…, Arterioscler Thromb Vasc Biol, 33(2):e47-55
Skånland et al., 2014, T-cell co-stimulation through the CD2 and CD28…, Biochem J, 460(3):399-410
Parente-Ribes et al., 2016, Spleen tyrosine kinase inhibitors reduce…, Haematologica, 101(2):e59-62
Myklebust et al., 2017, Distinct patterns of B-cell receptor signaling in…, Blood, 129(6): 759-770
Myhrvold et al., 2018, Single cell profiling of phospho-protein levels in.., Oncotarget, 9(10):9273-9284

Click here to download Author License Agreement (ALA) ALA.pdf

jove JOURNAL OF VISUALIZED EXPERIMENTS
1 Alewife Center #200
Cambridge, MA 02140
tel. 617.945.9051
www.jove.com

ARTICLE AND VIDEO LICENSE AGREEMENT

Title of Article: Phospho Flow Cytometry with Fluorescent Cell Barcoding for Single Cell ...

Author(s): Signid S. Skånland

Item 1 (check one box): The Author elects to have the Materials be made available (as described at http://www.jove.com/author) via: [X] Standard Access [ ] Open Access

Item 2 (check one box):

[X] The Author is NOT a United States government employee.

[ ] The Author is a United States government employee and the Materials were prepared in the course of his or her duties as a United States government employee.

[ ] The Author is a United States government employee but the Materials were NOT prepared in the course of his or her duties as a United States government employee.

ARTICLE AND VIDEO LICENSE AGREEMENT

1. Defined Terms. As used in this Article and Video License Agreement, the following terms shall have the following meanings: "**Agreement**" means this Article and Video License Agreement; "**Article**" means the article specified on the last page of this Agreement, including any associated materials such as texts, figures, tables, artwork, abstracts, or summaries contained therein; "**Author**" means the author who is a signatory to this Agreement; "**Collective Work**" means a work, such as a periodical issue, anthology or encyclopedia, in which the Materials in their entirety in unmodified form, along with a number of other contributions, constituting separate and independent works in themselves, are assembled into a collective whole; "**CRC License**" means the Creative Commons Attribution-Non Commercial-No Derivs 3.0 Unported Agreement, the terms and conditions of which can be found at: http://creativecommons.org/licenses/by-nc-nd/3.0/legalcode; "**Derivative Work**" means a work based upon the Materials or upon the Materials and other pre-existing works, such as a translation, musical arrangement, dramatization, fictionalization, motion picture version, sound recording, art reproduction, abridgment, condensation, or any other form in which the Materials may be recast, transformed, or adapted; "**Institution**" means the institution, listed on the last page of this Agreement, by which the Author was employed at the time of the creation of the Materials; "**JoVE**" means MyJove Corporation, a Massachusetts corporation and the publisher of *The Journal of Visualized Experiments;* "**Materials**" means the Article and / or the Video; "**Parties**" means the Author and JoVE; "**Video**" means any video(s) made by the Author, alone or in conjunction with any other parties, or by JoVE or its affiliates or agents, individually or in collaboration with the Author or any other parties, incorporating all or any portion of the Article, and in which the Author may or may not appear.

2. Background. The Author, who is the author of the Article, in order to ensure the dissemination and protection of the Article, desires to have the JoVE publish the Article and create and transmit videos based on the Article. In furtherance of such goals, the Parties desire to memorialize in this Agreement the respective rights of each Party in and to the Article and the Video.

3. Grant of Rights in Article. In consideration of JoVE agreeing to publish the Article, the Author hereby grants to JoVE, subject to **Sections 4** and **7** below, the exclusive, royalty-free, perpetual (for the full term of copyright in the Article, including any extensions thereto) license (a) to publish, reproduce, distribute, display and store the Article in all forms, formats and media whether now known or hereafter developed (including without limitation in print, digital and electronic form) throughout the world, (b) to translate the Article into other languages, create adaptations, summaries or extracts of the Article or other Derivative Works (including, without limitation, the Video) or Collective Works based on all or any portion of the Article and exercise all of the rights set forth in (a) above in such translations, adaptations, summaries, extracts, Derivative Works or Collective Works and (c) to license others to do any or all of the above. The foregoing rights may be exercised in all media and formats, whether now known or hereafter devised, and include the right to make such modifications as are technically necessary to exercise the rights in other media and formats. If the "Open Access" box has been checked in **Item 1** above, JoVE and the Author hereby grant to the public all such rights in the Article as provided in, but subject to all limitations and requirements set forth in, the CRC License.

4. Retention of Rights in Article. Notwithstanding the exclusive license granted to JoVE in **Section 3** above, the Author shall, with respect to the Article, retain the non-exclusive right to use all or part of the Article for the non-commercial purpose of giving lectures, presentations or teaching classes, and to post a copy of the Article on the Institution's website or the Author's personal website, in each case provided that a link to the Article on the JoVE website is provided and notice of JoVE's copyright in the Article is included. All non-copyright intellectual property rights in and to the Article, such as patent rights, shall remain with the Author.

5. Grant of Rights in Video – Standard Access. This **Section 5** applies if the "Standard Access" box has been checked in **Item 1** above or if no box has been checked in **Item 1** above. In consideration of JoVE agreeing to produce, display or otherwise assist with the Video, the Author hereby acknowledges and agrees that, Subject to **Section 7** below, JoVE is and shall be the sole and exclusive owner of all rights of any nature, including, without limitation, all copyrights, in and to the Video. To the extent that, by law, the Author is deemed, now or at any time in the future, to have any rights of any nature in or to the Video, the Author hereby disclaims all such rights and transfers all such rights to JoVE.

6. Grant of Rights in Video – Open Access. This **Section 6** applies only if the "Open Access" box has been checked in **Item 1** above. In consideration of JoVE agreeing to produce, display or otherwise assist with the Video, the Author hereby grants to JoVE, subject to **Section 7** below, the exclusive, royalty-free, perpetual (for the full term of copyright in the Article, including any extensions thereto) license (a) to publish, reproduce, distribute, display and store the Video in all forms, formats and media whether now known or hereafter developed (including without limitation in print, digital and electronic form) throughout the world, (b) to translate the Video into other languages, create adaptations, summaries or extracts of the Video or other Derivative Works or Collective Works based on all or any portion of the Video and exercise all of the rights set forth in (a) above in such translations, adaptations, summaries, extracts, Derivative Works or Collective Works and (c) to license others to do any or all of the above. The foregoing rights may be exercised in all media and formats, whether now known or hereafter devised, and include the right to make such modifications as are technically necessary to exercise the rights in other media and formats. For any Video to which this Section 6 is applicable, JoVE and the Author hereby grant to the public all such rights in the Video as provided in, but subject to all limitations and requirements set forth in, the CRC License.

7. Government Employees. If the Author is a United States government employee and the Article was prepared in the course of his or her duties as a United States government employee, as indicated in **Item 2** above, and any of the licenses or grants granted by the Author hereunder exceed the scope of the 17 U.S.C. 403, then the rights granted hereunder shall be limited to the maximum rights permitted under such statute. In such case, all provisions contained herein that are not in conflict with such statute shall remain in full force and effect, and all provisions contained herein that do so conflict shall be deemed to be amended so as to provide to JoVE the maximum rights permissible within such statute.

8. Likeness, Privacy, Personality. The Author hereby grants JoVE the right to use the Author's name, voice, likeness, picture, photograph, image, biography and performance in any way, commercial or otherwise, in connection with the Materials and the sale, promotion and distribution thereof. The Author hereby waives any and all rights he or she may have, relating to his or her appearance in the Video or otherwise relating to the Materials, under all applicable privacy, likeness, personality or similar laws.

9. Author Warranties. The Author represents and warrants that the Article is original, that it has not been published, that the copyright interest is owned by the Author (or, if more than one author is listed at the beginning of this Agreement, by such authors collectively) and has not been assigned, licensed, or otherwise transferred to any other party. The Author represents and warrants that the author(s) listed at the top of this Agreement are the only authors of the Materials. If more than one author is listed at the top of this Agreement and if any such author has not entered into a separate Article and Video License Agreement with JoVE relating to the Materials, the Author represents and warrants that the Author has been authorized by each of the other such authors to execute this Agreement on his or her behalf and to bind him or her with respect to the terms of this Agreement as if each of them had been a party hereto as an Author. The Author warrants that the use, reproduction, distribution, public or private performance or display, and/or modification of all or any portion of the Materials does not and will not violate, infringe and/or misappropriate the patent, trademark, intellectual property or other rights of any third party. The Author represents and warrants that it has and will continue to comply with all government, institutional and other regulations, including, without limitation all institutional, laboratory, hospital, ethical, human and animal treatment, privacy, and all other rules, regulations, laws, procedures or guidelines, applicable to the Materials, and that all research involving human and animal subjects has been approved by the Author's relevant institutional review board.

10. JoVE Discretion. If the Author requests the assistance of JoVE in producing the Video in the Author's facility, the Author shall ensure that the presence of JoVE employees, agents or independent contractors is in accordance with the relevant regulations of the Author's institution. If more than one author is listed at the beginning of this Agreement, JoVE may, in its sole discretion, elect not take any action with respect to the Article until such time as it has received complete, executed Article and Video License Agreements from each such author. JoVE reserves the right, in its absolute and sole discretion and without giving any reason therefore, to accept or decline any work submitted to JoVE. JoVE and its employees, agents and independent contractors shall have

full, unfettered access to the facilities of the Author or of the Author's institution as necessary to make the Video, whether actually published or not. JoVE has sole discretion as to the method of making and publishing the Materials, including, without limitation, to all decisions regarding editing, lighting, filming, timing of publication, if any, length, quality, content and the like.

11. Indemnification. The Author agrees to indemnify JoVE and/or its successors and assigns from and against any and all claims, costs, and expenses, including attorney's fees, arising out of any breach of any warranty or other representations contained herein. The Author further agrees to indemnify and hold harmless JoVE from and against any and all claims, costs, and expenses, including attorney's fees, resulting from the breach by the Author of any representation or warranty contained herein or from allegations or instances of violation of intellectual property rights, damage to the Author's or the Author's institution's facilities, fraud, libel, defamation, research, equipment, experiments, property damage, personal injury, violations of institutional, laboratory, hospital, ethical, human and animal treatment, privacy or other rules, regulations, laws, procedures or guidelines, liabilities and other losses or damages related in any way to the submission of work to JoVE, making of videos by JoVE, or publication in *JoVE* or elsewhere by JoVE. The Author shall be responsible for, and shall hold JoVE harmless from, damages caused by lack of sterilization, lack of cleanliness or by contamination due to the making of a video by JoVE its employees, agents or independent contractors. All sterilization, cleanliness or decontamination procedures shall be solely the responsibility of the Author and shall be undertaken at the Author's expense. All indemnifications provided herein shall include JoVE's attorney's fees and costs related to said losses or damages. Such indemnification and holding harmless shall include such losses or damages incurred by, or in connection with, acts or omissions of JoVE, its employees, agents or independent contractors.

12. Fees. To cover the cost incurred for publication, JoVE must receive payment before production and publication the Materials. Payment is due in 21 days of invoice. Should the Materials not be published due to an editorial or production decision, these funds will be returned to the Author. Withdrawal by the Author of any submitted Materials after final peer review approval will result in a US$1,200 fee to cover pre-production expenses incurred by JoVE. If payment is not received by the completion of filming, production and publication of the Materials will be suspended until payment is received.

13. Transfer, Governing Law. This Agreement may be assigned by JoVE and shall inure to the benefits of any of JoVE's successors and assignees. This Agreement shall be governed and construed by the internal laws of the Commonwealth of Massachusetts without giving effect to any conflict of law provision thereunder. This Agreement may be executed in counterparts, each of which shall be deemed an original, but all of which together shall be deemed to me one and the same agreement. A signed copy of this Agreement delivered by facsimile, e-mail or other means of electronic transmission shall be deemed to have the same legal effect as delivery of an original signed copy of this Agreement.

A signed copy of this document must be sent with all new submissions. Only one Agreement required per submission.

CORRESPONDING AUTHOR:

Name: SIGRID S. SKÅNLAND
Department: CENTRE FOR MOLECULAR MEDICINE NORWAY (NCMM)
Institution: UNIVERSITY OF OSLO
Article Title: PHOSPHO FLOW CYTOMETRY WITH FLUORESCENT CELL...
Signature: Sigrid S. Skånland
Date: 30/4-2018

Please submit a signed and dated copy of this license by one of the following three methods:

1) Upload a scanned copy of the document as a pfd on the JoVE submission site;
2) Fax the document to +1.866.381.2236;
3) Mail the document to JoVE / Attn: JoVE Editorial / 1 Alewife Center #200 / Cambridge, MA 02139

For questions, please email submissions@jove.com or call +1.617.945.9051

Centre for Molecular Medicine Norway
Nordic EMBL Partnership for Molecular Medicine

JoVE
Editor-in-Chief

Sigrid S. Skånland
PhD
t. +47 22859128
m. +47 98604333
sigrid.skanland@ncmm.uio.no

Date: 12. June 2018

RE: Revision of manuscript JoVE58386_R1

Dear Editor,

Thank you for you thorough revision of the manuscript JoVE58386 entitled *"Phospho Flow Cytometry with Fluorescent Cell Barcoding for Single Cell Signaling Analysis and Biomarker Discovery".* It is a great pleasure to learn that the manuscript will be acceptable for publication in *JoVE* pending minor revision based on editorial comments.

Response to the editorial comments can be found below. A few minor corrections to the manuscript text have also been included, and are highlighted in the submitted file.

Hopefully the Editors will appreciate the revised manuscript and it will now be appropriate for publication in *JoVE*.

Looking forward to hearing from you at your earliest convenience.

Yours Sincerely,

Sigrid S. Skånland

Sigrid S. Skånland, PhD

Responses to Editorial comments:

1. The references have been renumbered in order of appearance in the manuscript.

2. Figures 1D-1F are modified from the publication Myhrvold et al., *Oncotarget*, 2018. *Oncotarget* is an open-access journal which explicitly states on the first page of the article: *"This is an open-access article distributed under the terms of the Creative Commons Attribution License 3.0 (CC BY 3.0), which permits unrestricted use, distribution, and reproduction in any medium, provided the original author and source are credited.".* Since the source of Figures 1D-1F is clearly referenced, no additional reprint permission should be necessary. A copy of the original article with the copyright statement highlighted is enclosed in the re-submission.

3. The editor suggests separating Figure 1 into several figures. However, it is preferred to keep it as it is.

4. In the protocol, Alexa Fluor 647 is conjugated to the phospho-specific antibodies. Alexa Fluor 488 is used as a barcoding reagent. The indicated conflict regarding this in the manuscript could not be identified.

Supplemental File (Figures, Permissions, etc.)

Click here to download Supplemental File (Figures, Permissions, etc.) Myhrvold et al 2018.pdf

www.impactjournals.com/oncotarget/ Oncotarget, 2018, Vol. 9, (No. 10), pp: 9273-9284

Research Paper

Single cell profiling of phospho-protein levels in chronic lymphocytic leukemia

Ida K. Myhrvold[1,2,3], Andrea Cremaschi[1,4], Johanne U. Hermansen[1,2,3], Geir E. Tjønnfjord[5,7], Ludvig A. Munthe[6,7], Kjetil Taskén[1,2,3,8] and Sigrid S. Skånland[1,2,3]

[1]Centre for Molecular Medicine Norway, Nordic EMBL Partnership, University of Oslo and Oslo University Hospital, Oslo, Norway

[2]K. G. Jebsen Centre for Inflammation Research, University of Oslo, Oslo, Norway

[3]K. G. Jebsen Centre for Cancer Immunotherapy, University of Oslo, Oslo, Norway

[4]Oslo Centre for Biostatistics and Epidemiology (OCBE), University of Oslo, Oslo, Norway

[5]Department of Haematology, Oslo University Hospital, Oslo, Norway

[6]Centre for Immune Regulation, Department of Immunology, University of Oslo, Oslo University Hospital, Oslo, Norway

[7]Institute of Clinical Medicine, University of Oslo, Oslo, Norway

[8]Department of Infectious Diseases, Oslo University Hospital, Oslo, Norway

Correspondence to: Sigrid S. Skånland, **email:** sigrid.skanland@ncmm.uio.no

Keywords: *chronic lymphocytic leukemia; phospho-specific flow cytometry; signaling; STAT3*

Received: *April 28, 2017* ***Accepted:*** *November 16, 2017* ***Published:*** *January 04, 2018*

Copyright: Myhrvold et al. This is an open-access article distributed under the terms of the Creative Commons Attribution License 3.0 (CC BY 3.0), which permits unrestricted use, distribution, and reproduction in any medium, provided the original author and source are credited.

ABSTRACT

Chronic lymphocytic leukemia (CLL) has a high incidence and a steeply growing prevalence in the Western world. The heterogeneity of the disease necessitates individual mapping of biology and predicted drug response in each patient as basis for administration of tailored treatments. Cell signaling aberrations may serve as biological indicators for suitable therapy. By applying phospho-specific flow cytometry, we mapped basal and induced phosphorylation levels of 20 phospho-epitopes on proteins relevant to B-cell signaling in B cells from 22 CLL patients and 25 normal controls. The signaling response of the cytostatic drugs fludarabine, doxorubicin and vincristine was also investigated. CLL cells exerted similar or lower basal phosphorylation levels compared to normal B cells, with the exception of STAT3 (pY705) which was increased. Interestingly, STAT3 inhibitors normalized the STAT3 (pY705) level and reduced cell viability. Vincristine treatment significantly modulated phosphorylation levels in CLL cells, while no effect was observed in controls or after fludarabine or doxorubicin treatment. After BCR stimulation, CLL cells showed a tendency towards impaired phosphorylation levels, significant for several of the analyzed proteins. However, the level of Akt (pS473) was more potently induced in *IgHV* unmutated CLL (UM-CLL) patient samples and was significantly higher than in M-CLL samples. Importantly, the PI3Kδ inhibitor idelalisib potently reversed the effect of anti-IgM on Akt (pS473). Thus, signaling aberrations could be identified by phosphoflow cytometry and aberrant signaling could be normalized by small molecule drugs. This approach can identify relevant drug targets as well as drug effects in the individual patient.

INTRODUCTION

Chronic lymphocytic leukemia (CLL) is one of the most prevalent B-cell neoplasias in the Western world [1]. The heterogeneity of the disease results in variable clinical courses with survival ranging from one to more than 15 years [2]. Several molecular and cellular markers have been identified as prognostic markers and can predict disease progression. In particular, immunoglobulin heavy-chain variable gene (IgHV) mutational status,

chromosomal abnormalities and expression of CD38 and Zeta-chain-associated protein kinase of 70 kDa (ZAP70) are well established markers [3].

The B cell receptor (BCR) pathway with its associated signaling proteins is essential for normal immune function and for survival and proliferation of B cells. The mutational status of the IgHV is a strong predictor for disease outcome in CLL, suggesting that signaling through the BCR plays an important role in CLL pathogenesis [4]. The BCR is composed of covalently linked immunoglobulin heavy and light chains and is tightly associated with the membrane integrated CD79a and b. After antigen stimulation, the BCR aggregates, and the CD79a/b propagate an activation signal to a Sarcoma (Src)-family protein tyrosine kinase, normally Lyn (see Figure 5C for a simplified cartoon of BCR signaling), which then induces phosphorylation of the immunoreceptor tyrosine-based activation motifs (ITAMs) on CD79a and b. The phosphorylated ITAMs serve as docking sites for SH2-domain containing proteins, most often Spleen tyrosine kinase (SYK). There is some redundancy in signaling, ZAP70, which is highly expressed in CLL cells with an aggressive course, may also contribute [5]. The signaling continues with formation of the BCR signalosome and the recruitment of B cell linker protein (BLNK) to CD79b. BLNK serves as a docking site for Bruton's tyrosine kinase (Btk), Phospholipase Cγ2 (PLCγ2) and the adaptor protein Growth factor receptor-bound protein 2 (GRB2). This BCR signalosome generates a wide variety of downstream effects, including activation of the PI3K-Akt-mTOR pathway and the Ras-Raf-MEK-ERK pathway [6].

After assembly of the BCR signalosome, signaling through GRB2, the Son of sevenless (SOS) and rat sarcoma protein (Ras) is propagated downstream leading to activation of the Raf proto-oncogene serine/threonine-protein kinase (Raf), followed by Mitogen activated protein kinase kinase (MEK), and Mitogen activated protein kinase (p44/42 MAPK/ERK1/2). This Ras-Raf-MEK-ERK pathway regulates the expression of the Activator protein 1 (AP1) which is a transcription factor important for proliferation and differentiation [6].

The PI3K-Akt-mTOR pathway is involved in many cellular functions, including cell cycle progression, cell survival and apoptosis. It is one of the most commonly mutated pathways in cancer, and increased activity of this pathway has been observed in many malignancies, including leukemias [4]. After BCR activation, the PI3K converts phosphatidylinositol-4,5-bisphosphate (PIP2) to phosphatidylinositol-3,4,5-trisphosphate (PIP3), which serves as a membrane docking site for the plextrin homology (PH) domains in Akt and Phosphoinositide-dependent protein kinase 1 (PDK1). Mammalian target of rapamycin (mTOR) is recruited, and both mTOR and PDK1 phosphorylate Akt. Fully activated Akt phosphorylates various target proteins, leading to inhibition of apoptosis and promotion of cell survival [4].

A central signaling pathway in CLL is the JAK/STAT pathway [7]. Activation of this pathway stimulates cell migration, proliferation, differentiation and apoptosis which are crucial for growth and development of the immune system [8]. When a ligand, such as a growth hormone or a cytokine like Interferon γ (IFNγ), binds to its cognate receptor, a receptor dimer is formed and Janus kinase (JAK) tyrosine kinases are recruited. The JAKs phosphorylate additional targets, including the STATs. The STATs are latent transcription factors ready to activate or repress transcription of target genes, including CD38 [7, 8].

Here, basal and induced signaling in CLL cells relative to normal controls were analyzed by phosphoflow cytometry in order to map signaling aberrations that can provide indications for targeted therapy. Furthermore, the signaling responses of the purine analogue fludarabine, the vinca alkaloid vincristine and the anthracycline doxorubicin were characterized. These cytostatic drugs are currently in use for the treatment of CLL [9]. However, their effects on signaling responses have to our knowledge not previously been characterized in detail. The present study suggests that phosphoflow cytometry has the potential to identify relevant drug targets as well as drug effects in the individual patient.

RESULTS

Characterization of basal phosphorylation levels in CLL and normal B cells

In order to identify signaling aberrations in CLL cells relative to normal B cells, we investigated both basal and induced phosphorylation levels of 20 different phospho-epitopes on signaling proteins relevant for the BCR signaling pathway.

When the phospho-protein levels in 22 CLL samples were analyzed relative to the mean of normal controls, the basal phosphorylation levels were shown to be reduced and significantly different ($p \in 0.0001$-0.05) for the phospho-proteins BLNK (pY84), Btk (pY551) & Itk (pY511), MEK1 (pS298), S6-Ribosomal protein (pS235/236) and STAT6 (pY641). MAPKAPK-2 (pT334) and STAT3 (pY705) were increased and statistically different from controls ($p < 0.001$) (Figure 1A). Nine patient samples, including both UM-CLL and M-CLL type, showed more than two-fold increase in STAT3 (pY705) level relative to controls. By using an agglomerative hierarchical clustering procedure (Euclidean distance – Ward's linkage method) on the CLL samples, the STAT3 (pY705)-high samples were grouped into two distinct clusters (indicated in pink and blue in Figure 1B). The two clusters suggest similar signaling patterns among the patients, with the larger group being characterized by higher STAT3 (pY705) levels (pink in Figure 1A and 1B. See also Figure 4C). Supplementary Figure 1 shows the non-

normalized phospho-protein levels in both CLL samples and normal controls. Unpaired two-samples *t*-test was used to assess the difference between the CLL and normal samples, with *p* values corrected for multiple comparisons using Holm-Sidak's method (Supplementary Figure 1A). In Supplementary Figure 1B, data for 18 out of the 20 non-normalized phospho-proteins were used to perform an agglomerative hierarchical clustering (Euclidean distance – average linkage method) of both CLL and normal B cells ($n = 10$, see Figure 4C). For this analysis, STAT6 (pY641) was removed due to the presence of several missing values, as well as MAPKAPK-2 (pT334) since its high values reduced the visibility of the variability of the data. Log-transformation was then applied to further emphasize the differences in the signals. In this analysis, several of the STAT3 (pY705)-high samples still grouped together, but not to the same extent as observed in Figure 1B (Supplementary Figure 1B).

In Figure 1C, the correlation between the phospho-proteins in unstimulated CLL samples was investigated. The correlation coefficient ranges from -1 (dark red) to +1 (dark blue). The diagonal of the matrix separates the lower left triangle which shows the sample correlations for all phospho-protein pairs from the upper right triangle which shows the significant correlations only (p-value < 0.05) (Figure 1C). As expected, the two phospho-epitopes on NF-κB p65 (pS529 and pS536) displayed a positive correlation of approximately +1. Furthermore, the proteins BLNK (pY84), Btk (pY551) Itk (pY511), and PLCγ2 (pY759), which are part of the BCR signalosome, also showed positive correlation (Figure 1C). STAT3 (pY705) showed significant positive correlation only with STAT1 (pY701) and NF-κB p65 (pS529). The correlation patterns could also be visualized in Figure 1A. For example, the majority of the STAT3 (pY705) high samples showed high levels of STAT1 (pY701) and NF-κB p65 (pS529). In agreement with the correlation data, STAT3 signaling has been reported to be highly interconnected with NF-κB signaling [10].

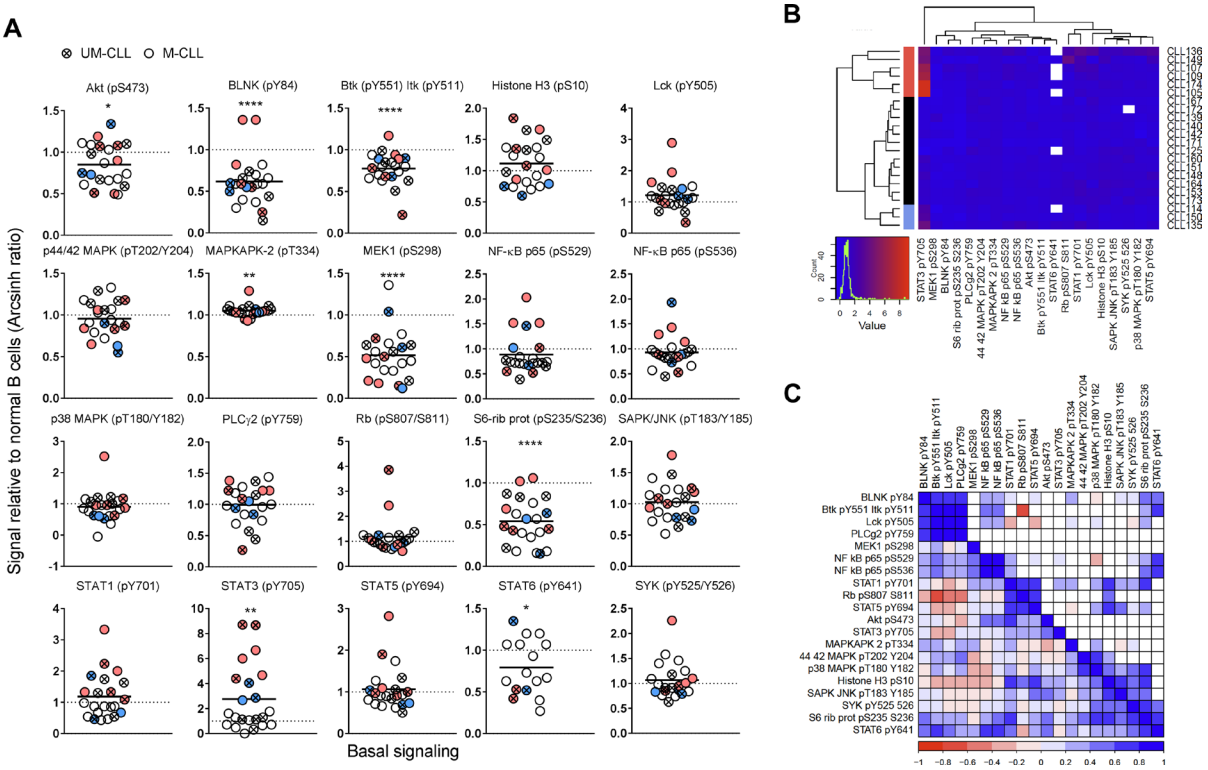

Figure 1: Basal phospho-protein levels in CLL B cells. (**A**) Unstimulated B cells from healthy donors ($n = 25$) and CLL patients ($n = 22$) were fixed, permeabilized and stained with anti-CD19 surface marker and indicated phospho-protein specific antibodies as described in Materials and Methods. The fluorescence signals were detected by flow cytometry and the data were analyzed in Cytobank. The basal fluorescence intensity signals were calculated relative to IgGκ isotype control and shown as arcsinh ratio. The relative phospho-protein levels in CLL B cells were normalized to normal controls. Significant *p*-values are indicated ($^{*}p < 0.05$, $^{**}p < 0.01$, $^{***}p < 0.001$, $^{****}p < 0.0001$), and were calculated by unpaired two-samples *t*-test. Symbols with a cross represent UM-CLL patient samples, while open circles represent M-CLL patient samples. Pink and blue symbols refer to STAT3 (pY705) high samples which cluster together (see B). Horizontal bars indicate calculated mean. (**B**) Phospho-proteins and CLL samples shown in (A) were grouped via hierarchical agglomerative clustering (linkage method used was Ward's method). Missing data points are shown in white. Pink and blue clusters indicate patient samples with high level of STAT3 (pY705) (see A). (**C**) Matrix comparing paired phospho-protein sample correlations in CLL samples (lower left triangle, $n = 22$). Higher correlation is indicated by darker colour (red for negative, blue for positive). Upper right triangle shows only those entries associated with correlations significantly different from 0 (assessed by using Pearson's r-test, *p*-value < 0.05).

Briefly, aberrant levels of protein phosphorylation were identified in unstimulated CLL cells and a group of samples showed elevated STAT3 (pY705) as well as a similar signaling pattern overall.

STAT3 inhibitors normalize aberrant STAT3 signaling and reduce cell viability in CLL

Of clinical significance, STAT3 has been reported to be constitutively active in a large number of cancers including haematological malignancies. However, this characteristic has not previously been shown to comprise CLL [11]. Due to its therapeutic significance, STAT3 is the target in numerous drug discovery research efforts. As shown in Figure 2, the STAT3 inhibitors niclosamide and WP1066 significantly reduced both STAT3 (pY705) levels (Figure 2A) and cell viability (Figure 2B, 2C) of CLL cells in a concentration-dependent manner. Of notice, the ATP-based assay CellTiter-Glo detected drug effects at lower drug concentrations than the Annexin V/PI based assay (Figure 2B, C and data not shown), suggesting that the STAT3 inhibitors reduce cellular metabolism before cell death is induced. These findings indicate that STAT3 signaling is implicated in CLL cell viability, and that the protein may represent a potential therapeutic target. However, additional studies are required in order to conclude whether phospho-flow profiling can predict the response to STAT3 inhibitors.

Phospho-flow profile of STAT3 inhibitors reveal multiple signaling effects

In addition to the observed and expected inhibition of STAT3 phosphorylation, a full phospho-flow profiling was carried out using the two STAT3 inhibitors. CLL cells were exposed to a concentration range (ten-fold steps from 1 nM to 10 μM) of niclosamide or WP1066 for 20 min before signaling patterns were analyzed. The results using 10 μM of each drug is shown in Figure 3. Both STAT3 inhibitors induced a significant reduction in Akt (pS473), Lck (pY505), STAT5 (pY694) and SYK (pY525/Y526). Furthermore, both drugs caused additional specific signaling deviations (Figures 3 and 5C). Results suggest that STAT3 inhibitors alter the phosphorylation status of multiple signaling molecules.

Distinct BCR signaling patterns in CLL and normal B cells

To identify any signaling differences induced through the BCR pathway in CLL cells relative to normal B cells, the cells were next stimulated with anti-IgM and followed for 30 min (Figure 4). It has previously been reported that UM-CLL cells show an increased sensitivity towards anti-IgM stimulation [12]. We observed that UM-CLL cells exhibited a tendency towards higher phospho-protein levels relative to M-CLL cells for the majority of the analyzed proteins, but the effect was statistically significant for Akt (pS473) only (Figure 4A, 4B). For this parameter the phosphorylation-levels in UM-CLL cells also significantly exceeded those detected in normal controls (Figure 4A and 4B). In general, however, the CLL cells were hyporesponsive or showed only minor deviations from normal B cells (Figure 4A and 4B).

The exact cellular origin for CLL cells is still under debate [13], a possible confounding influence in the current results was the choice of normal control cells. These were predominately $CD19^+$ B cells that lacked expression of CD5, a differentiation or activation marker of B cells. CLL cells are $CD5^+CD19^+$ cells, while the normal control cells were nearly all $CD5^-CD19^+$. An additional control was therefore included in which signaling patterns were compared between normal $CD5^-CD19^+$ and $CD5^+CD19^+$ cells. As shown in Supplementary Figure 2, no significant differences were observed between these subsets.

In order to investigate whether the signaling patterns in CLL samples could be separated from normal controls, an unsupervised cluster analysis based on phospho-epitope phosphorylation status after 5 min of anti-IgM stimulation was performed. Interestingly, the cluster analysis revealed that samples from healthy donors and CLL patients made up three separate clusters (Figure 4C). Two sub-clusters were observed for the CLL patients, but IgHV mutational status or other patient characteristics did not explain this separation. Interestingly, the STAT3 (pY705) high patient samples to some extent clustered together (Figure 4C). For the phospho-proteins examined, three sub-clusters were identified. One sub-cluster consisted of Akt (pS473) and S6-Ribosomal protein (pS235/S236). These two phospho-proteins showed distinct patterns in CLL samples relative to normal controls, most obviously so for Akt (pS473) which was higher in the CLL cells (Figure 4C). A second sub-cluster consisted of p44/42 MAPK (pT202/Y204), p38 MAPK (pT180/Y182), BLNK (pY84), Lck (pY505), SYK (pY525/Y526) and PLCγ2 (pY759). These phospho-proteins were all low in CLL samples and most of them were statistically different from the levels in normal controls (Figure 4C, 4B). The proteins in the remaining sub-cluster displayed similar levels among all donors (Figure 4C).

In order to investigate whether the aberrantly induced signaling observed in CLL cells could be reversed to normal levels, anti-IgM induced Akt (pS473) signaling was targeted using a range of concentrations of the PI3Kδ inhibitor idelalisib (Figure 4D). This drug is currently in use for treatment of CLL. All patient samples showed reduced Akt (pS473) levels after treatment with increasing concentrations of the drug (Figure 4D), demonstrating that pathway inhibitors can be applied to normalize aberrant signaling in CLL cells.

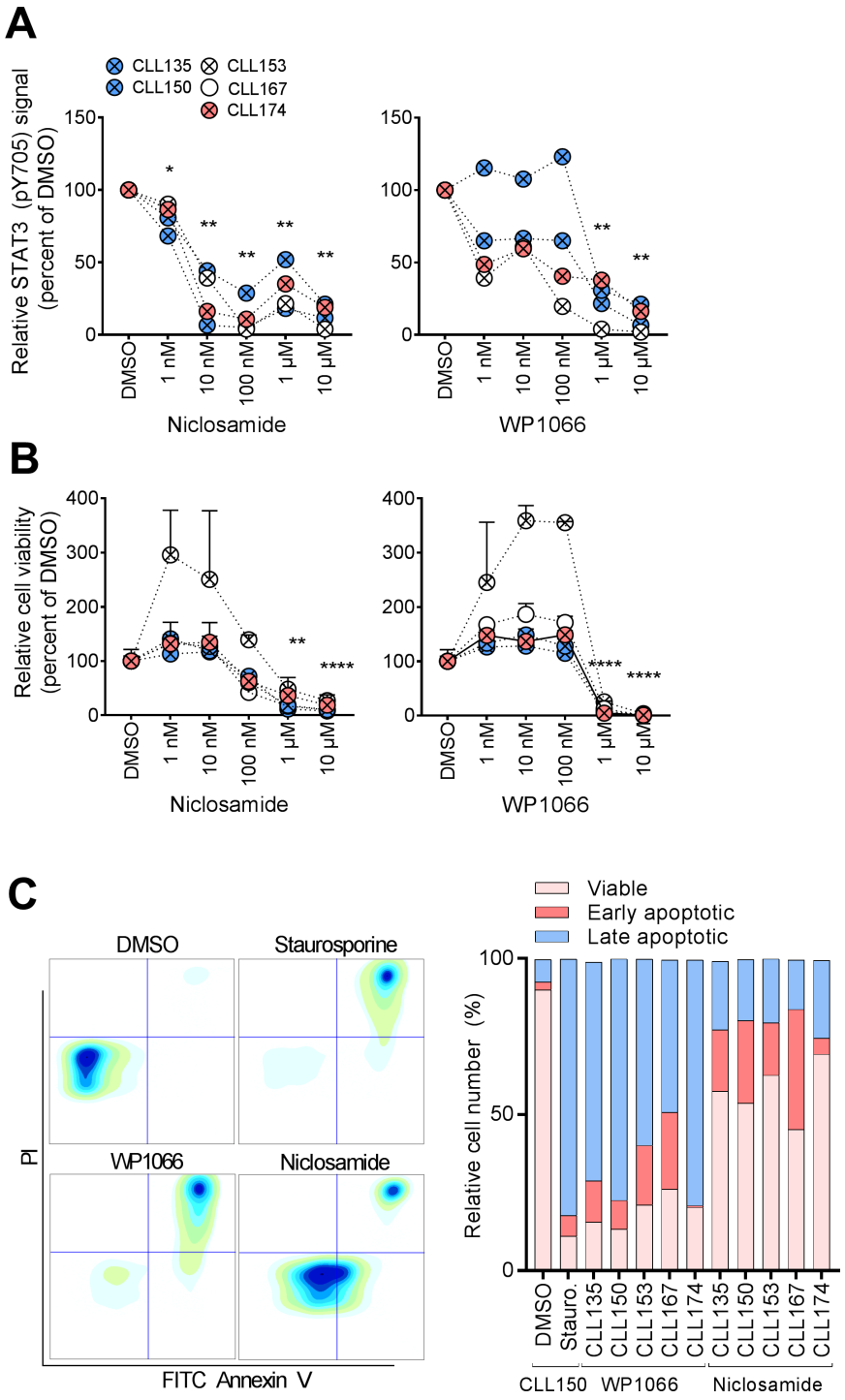

Figure 2: STAT3 inhibitors normalize aberrant CLL signaling. (**A**) B cells were incubated with DMSO or the indicated drug concentration for 24 hours, then fixed, barcoded and permeabilized before antibody staining and analysis as described in Materials and Methods. (**B**) CLL cells were co-cultured with CD40L+, BAFF+ and APRIL+ (ratio 1:1:1) L cells for 24 hours prior to initiation of the experiment to prevent induction of spontaneous apoptosis. The L cells were removed, and the CLL cells were incubated with the indicated drugs for 48 hours. CellTiter-Glo reagent was subsequently added and luminescence was recorded after 10 min incubation at room temperature using an EnVision 2102 Multilabel Reader. $N = 3$, SEM. P values were calculated by multiple comparison testing with Holm-Sidak's correction. Asterisks indicate significant p-value ($^{*}p < 0.05$, $^{**}p < 0.01$, $^{***}p < 0.001$, $^{****}p < 0.0001$). (**C**) CLL cells were cultured and exposed to drug (10 μM) as described above. Cells treated with staurosporine (1 μM) were included as a positive control. The cells were then stained with FITC Annexin V and PI, and analyzed by flow cytometry. Plots from one patient sample (CLL150) are shown (left). Relative numbers of viable cells (lower left gate), early apoptotic cells (lower right gate) and late apoptotic cells (upper right gate) are plotted for the indicated patient samples (graph, right).

Effects of cytostatic drugs on B cell signaling

The effects of the cytostatic drugs fludarabine, doxorubicin and vincristine on B cell signaling were investigated. These drugs are currently used in CLL therapy, but a detailed characterization of their effects on signaling in B cells has to our knowledge not previously been carried out. We chose to study the signaling effects induced by short-time (20 min) incubation with the drugs. In order to determine the optimal working concentrations of these drugs, normal B cells were treated with three different concentrations (0,1 μM, 1 μM and 10 μM) of the drugs, followed by anti-IgM stimulation (Figure 5A). The cells responded in a concentration-dependent manner to the drugs with the most pronounced effect at the highest concentration. However, doxorubicin appeared to be toxic to the B cells at 10 μM (Figure 5A, and data not shown). Based on these results, we chose the working concentrations 10 μM, 1 μM and 10 μM for fludarabine, doxorubicin and vincristine, respectively, which is in line with previous *in vitro* studies [14–16].

No significant changes in phosphorylation levels could be induced by any of the three drugs in B cells from healthy donors (data not shown). However, in CLL cells, some of the 20 investigated phospho-proteins were significantly modulated upon vincristine treatment, but not by fludarabine or doxorubicin (Figure 5B). The observed modifications included lowered Akt (pS473) and NF-κB

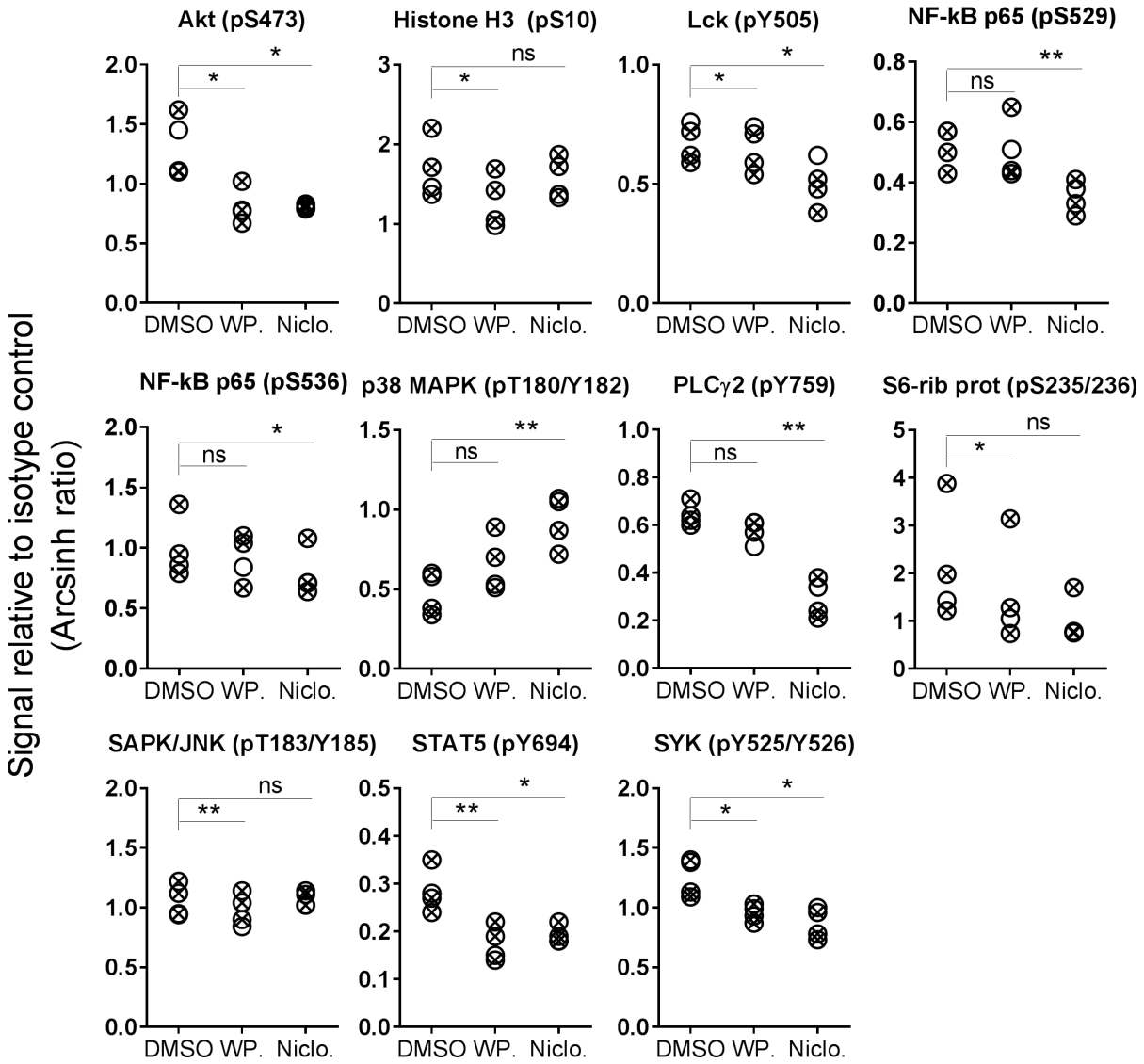

Figure 3: STAT3 inhibitor-induced phosphorylation levels in CLL B cells. CLL cells were incubated with DMSO (0.001%), WP1066 (WP.; 10 μM) or niclosamide (Niclo.; 10 μM) for 20 min. The cells were then processed and analyzed as described in Figure 1. Indicated *p*-values were calculated by multiple comparison testing with Holm-Sidak's correction ($^{*}p < 0.05$, $^{**}p < 0.01$, ns: not significant). Only phospho-proteins where at least one of the drugs induced significant changes are shown. Symbols with a cross represent UM-CLL samples, while open circles represent M-CLL samples.

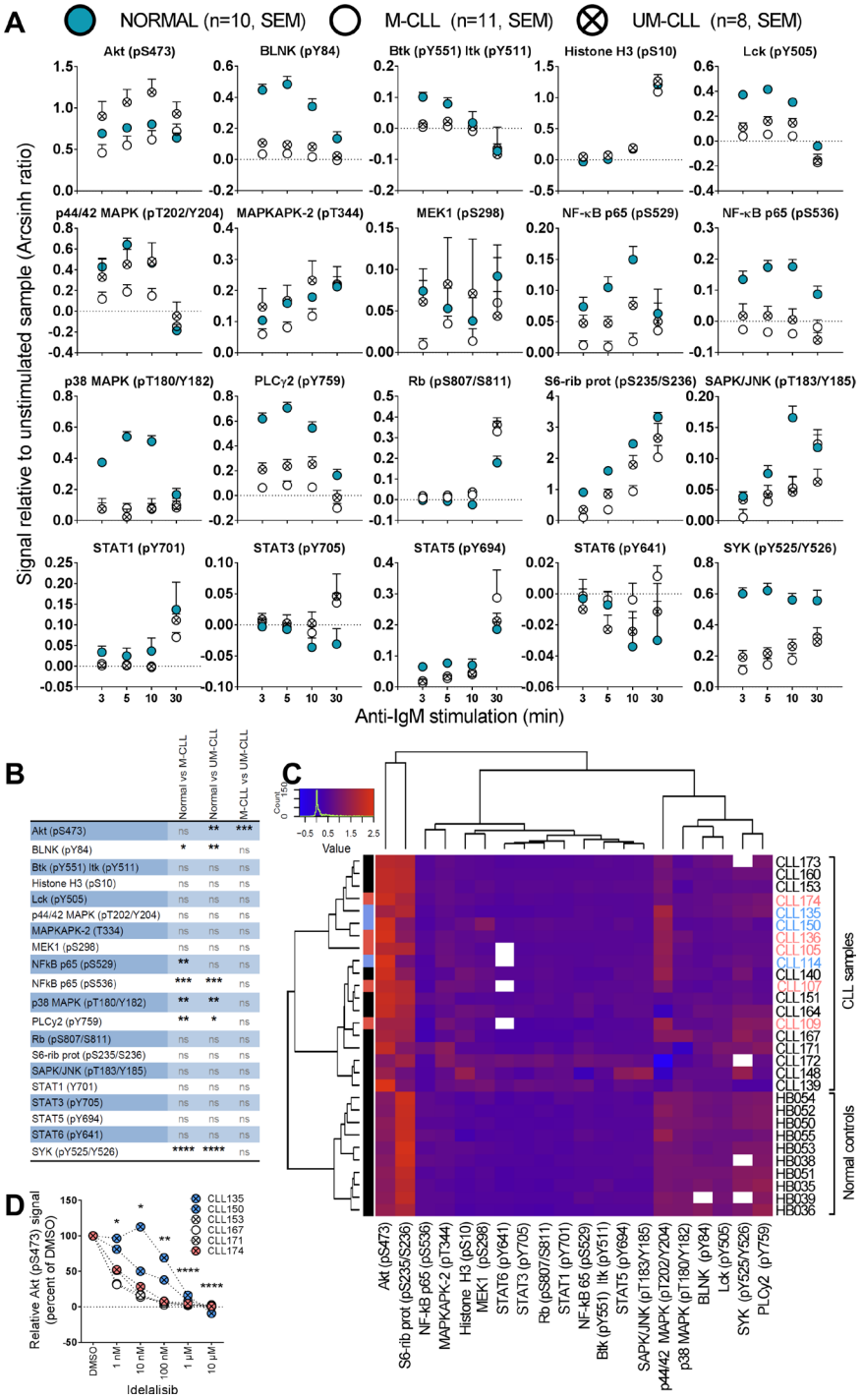

Figure 4: Anti-IgM induced signaling in B cells from healthy donors and CLL patients. (**A**) B cells from healthy donors (mean + SEM, $n = 10$, filled circles) or CLL patients (mean + SEM, $n = 11$ (M-CLL, open circles) and $n = 8$ (UM-CLL, crossed circles)) were stimulated with anti-IgM for the specified time period, then processed and analyzed as described in Figure 1. The fluorescence intensity signals were measured relative to unstimulated samples and shown as arcsinh ratio. (**B**) Summary of multiple comparison testing with Holm-Sidak's correction for normal, M-CLL and UM-CLL groups as shown in (A). Asterisks indicate significant p-value ($^{*}p < 0.05$, $^{**}p < 0.01$, $^{***}p < 0.001$, $^{****}p < 0.0001$), ns: not significant. (**C**) Phospho-proteins and B-cell samples shown in (A) were grouped via hierarchical agglomerative clustering (linkage method used was Ward's method), analogously to Figure 1B. The heatmap shows signals induced by anti-IgM stimulation for 5 min. Missing data are indicated in white. Patients highlighted in pink and blue refer to the STAT3 (pY705) high patients as shown in Figure 1. (**D**) B cells were incubated with DMSO or the indicated idelalisib concentration for 20 min before anti-IgM stimulation for 3 min. The cells were then fixed, barcoded and permeabilized before antibody staining and analysis as described in Materials and Methods. P values were calculated by multiple comparison testing with Holm-Sidak's correction. Asterisks indicate significant p-value ($^{*}p < 0.05$, $^{**}p < 0.01$, $^{***}p < 0.001$, $^{****}p < 0.0001$).

65 (p536) signals, and increased p38 MAPK (pT180/Y183) and SAPK/JNK (pT183/Y185) phosphorylation. However, although the modulations were statistically significant, the biological significance of these signaling effects need to be further investigated. It has previously been reported that vincristine induces SAPK/JNK activation in BR ovarian carcinoma cells and MCF-7 breast cancer cells [17]. No significant changes in phosphorylation levels were detected in cells treated with a cytostatic drug followed by anti-IgM stimulation (data not shown). A summary of the proteins which showed altered basal or drug-induced phosphorylation in CLL cells is shown in Figure 5C. All drugs that induced statistically significant signaling alterations are shown.

DISCUSSION

In the present study, basal and anti-IgM induced phospho-protein levels were characterized in B cells from healthy donors and CLL patients. The phosphorylation levels of 20 different phospho-epitopes on proteins downstream of the BCR were used as read-out in phospho-flow assays. In addition, the effects on signaling responses of the therapeutic cytostatic drugs fludarabine, doxorubicin and vincristine which are commonly used in CLL treatment were investigated. Here, phospho-flow was the method of choice to study CLL signaling. Other techniques such as protein array and reverse phase protein array (RPPA) may be used to quantify the expression levels of phospho-proteins in a medium to high-throughput manner. An important advantage of phospho-flow is that it is based on very versatile flow cytometry analysis that allows for characterization of single cell phenotype as well as detection of inter-cellular heterogeneity. In the present study, the multiplexing of the phospho-flow analysis allowed us to identify aberrations even in this early explorative phase with modest sample size. Our results suggest that more extensive future studies may define multiple targets in the heterogeneous CLL patient population.

Basal signaling in CLL was first investigated, and when the CLL patient samples were analyzed as one population, several deviations were detected relative to the normal control group. Most of these deviations showed lower basal signals in CLL cells, probably as a result of feedback inhibition. However, a significant increase in the basal level of STAT3 (pY705) was observed in about a third of the samples and both in UM-CLL and M-CLL samples. Constitutive serine phosphorylation of STAT1 and STAT3 has been reported in CLL cells, while tyrosine phosphorylation of these STAT proteins was not detected [18]. A recent study on signaling profiles in non-Hodgkin lymphomas suggested that basal STAT3 (pY705) levels were elevated in CLL cells relative to normal B cells, but the statistical significance was not indicated [19]. For other haematological malignancies, constitutive activation of STAT3 has been demonstrated [11]. Cancer cells with constitutive STAT3 activation have been reported to have elevated levels of cell cycle regulating and anti-apoptotic proteins, leading to resistance to apoptosis [11]. Importantly, the two experimental STAT3 inhibitors WP1066 and niclosamide reversed the elevated phosphorylation of STAT3 and reduced the viability of CLL cells. These results suggest that aberrant signaling can be targeted and modulated by drugs that specifically perturb signaling pathways to the extent that they may be applicable for future clinical testing.

A previous study on signaling in SLL/CLL cells [20] reported significantly higher basal phosphorylation levels of PLCγ2 (pY759), p44/42 MAPK (pT202/Y204), p38 MAPK (pT180/Y182), NF-κB p65 (pS529), STAT5 (pY694) and STAT6 (pY641) in these cells compared to normal B cells. In the present study, similar elevations in phosphorylation were not observed. Rather, a tendency towards lower basal phosphorylation levels in CLL cells was found, although outliers were present. The inconsistence between the two studies may possibly be due to different experimental approaches. Herein samples from CLL patients were investigated, whereas Blix et al. included samples from both CLL and small lymphocytic lymphoma (SLL) patients [20]. Although these diseases are considered to be similar, SLL B cells have a smaller leukemic subpopulation and reside more strictly at nodal sites [21]. Furthermore, the samples in the present study were obtained from blood whereas Blix et al. prepared single-cell suspensions from collected tumor biopsies [20].

When the effects of the cytostatic drugs fludarabine, doxorubicin and vincristine on cell signaling were investigated, a few significant signaling modulations were observed after vincristine treatment of CLL cells, while no effects were detected in normal B cells or after fludarabine or doxorubicin treatment. SAPK/JNK (pT183/Y185) phosphorylation was significantly increased in CLL patient samples after vincristine treatment. This finding is in line with a previous report where the effect of vincristine was examined in BR ovarian carcinoma cells and MCF-7 breast cancer cells [17]. Wang et al. reported that activation of SAPK/JNK increased in a dose-dependent manner after treatment with vincristine.

BCR signaling, induced after stimulation with anti-IgM for up to 30 minutes, was also characterized. Only Akt (pS473) showed higher phosphorylation-levels in UM-CLL cells relative to both M-CLL and normal B cells. The remaining significant differences indicated lower signaling amplitudes in CLL cells relative to normal B cells. Our observation of hypo-phosphorylation after BCR stimulation was in agreement with previous reports [19, 20].

In summary, basal and anti-IgM induced signaling was characterized in detail in B cells from healthy donors and CLL patients. Signaling aberrations in CLL cells may be used to guide targeted therapy. We recently showed that sCD40L stimulation more efficiently induced

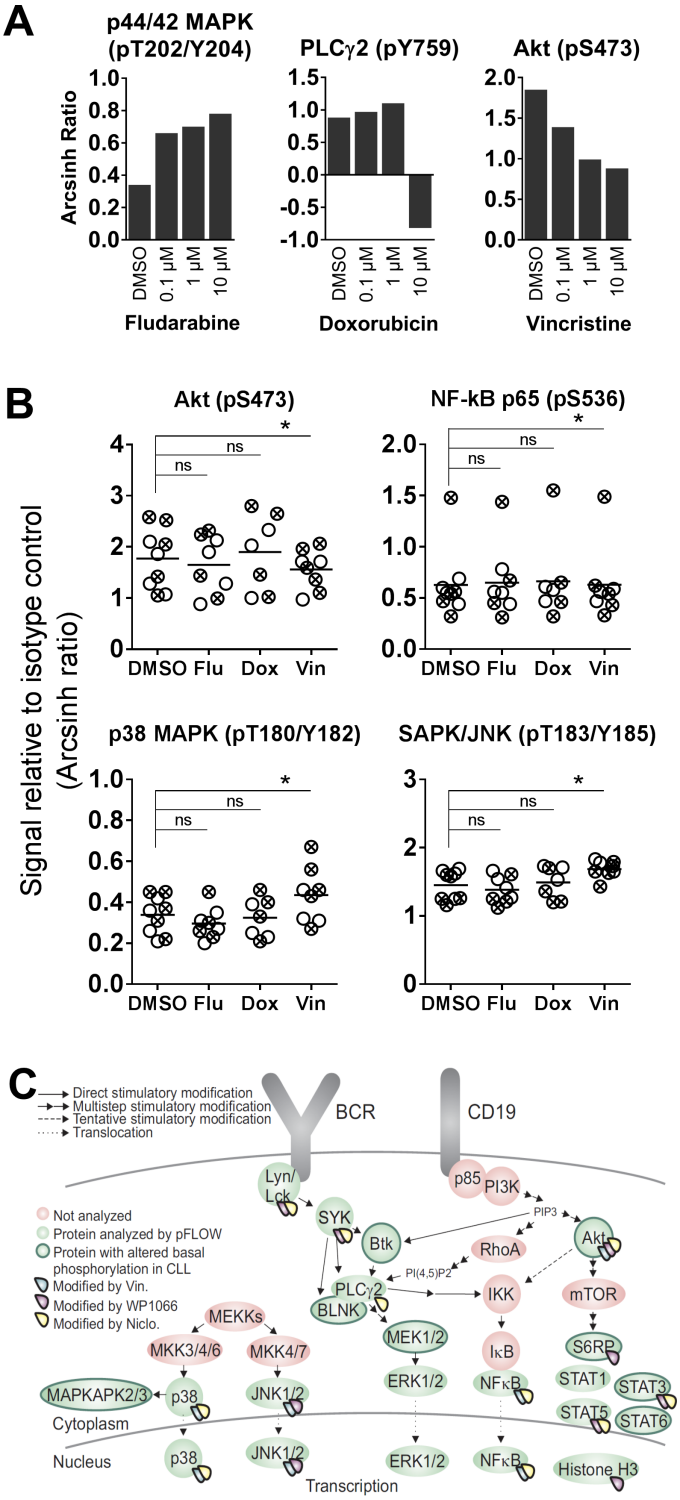

Figure 5: Cytostatic drug-induced phosphorylation levels in CLL B cells. (**A**) B cells from healthy donors were incubated with the indicated concentrations of fludarabine, doxorubicin or vincristine for 20 min, before stimulation with anti-IgM for 3 min. The cells were then processed as in Figure 1, and the fluorescence intensity signals were measured relative to unstimulated samples and shown as arcsinh ratio. (**B**) CLL cells were incubated with DMSO (0.001%), fludarabine (Flu; 10 μM), doxorubicin (Dox; 1 μM) or vincristine (Vin; 10 μM) for 20 min. The cells were then processed and analyzed as described in Figure 1. The DMSO data are from Figure 1A. Indicated *p*-values were calculated by multiple comparison testing with Holm-Sidak's correction ($^{*}p < 0.05$, ns: not significant). Only phospho-proteins where at least one of the drugs induced significant changes are shown. Symbols with a cross represent UM-CLL samples, while open circles represent M-CLL samples. Horizontal bars indicate calculated mean. (**C**) Illustration highlighting proteins that show significantly altered basal or drug-induced phosphorylation levels in CLL B cells relative to normal controls.

phosphorylation of SYK in CLL cells relative to normal B cells, and that SYK inhibitors reduced CD40L-induced proliferation of CLL cells specifically [22]. In the present study we showed that constitutive as well as induced signaling could be reversed by the use of specific pathway inhibitors. These findings demonstrated that signaling aberrations can be identified by phosphoflow cytometry, and that aberrant signaling could be normalized by small molecule drugs that perturbed specific signaling pathways. Results suggest clinical applications of such results and tests to the extent that such inhibitors are available clinically. This approach can thus identify relevant drug targets as well as drug effects in the individual patient.

MATERIALS AND METHODS

Patient material and ethical considerations

Buffy coats from anonymized healthy blood donors and blood samples from CLL patients were received from the Blood Centre (Oslo University Hospital) and the Department of Haematology, Oslo University Hospital, respectively, following written informed consent from all donors. Controls from the Blood Centre were drawn from a donor population where 45% were > 47 years of age. The study was approved by the Regional Committee for Medical and Health Research Ethics of South-East Norway and the research on human blood was carried out in accordance with the Declaration of Helsinki (2013). Clinical characteristics of the CLL patients included in this study are listed in Supplementary Table 1.

Reagents and antibodies

The cytostatic drugs fludarabine, doxorubicin and vincristine, the PI3Kδ inhibitor idelalisib (CAL-101) and the STAT3 inhibitors WP1066 and niclosamide were from Selleckchem (Houston, TX, USA). The alexa Fluor 647-conjugated antibodies BLNK (pY84), Btk (pY551) & Itk (pY511), IgGkappa, Lck (pY505), MEK1 (pS298), NF-κB p65 (pS529), PLCγ2 (pY759), Rb (pS807/811), STAT1 (pY701), STAT3 (pY705), STAT5 (pY694) and STAT6 (pY641) were from BD Biosciences (Franklin Lakes, NJ, USA). Alexa Fluor 647-conjugated antibodies against Akt (pS473), Histone H3 (pS10), MAPKAPK-2 (pT334), p44/42 MAPK (pT202/Y204), NF-κB p65 (pS536), p38 MAPK (pT180/Y182), SAPK/JNK (pT183/Y185), S6-Ribosomal protein kinase (pS235/236), and SYK (pY525/526) were from Cell Signaling (Danvers, MA, USA). The anti-human surface marker PerCP-Cy5.5-conjugated CD19 was from eBioscience (San Diego, CA, USA) and anti-human PE-Cy7-conjugated CD5 was from BD Biosciences. Anti-human IgM was from Southern Biotech (Birmingham, AL, USA). The RosetteSep Human B Cell Enrichment Cocktail and Lymphoprep were from Stemcell Technologies (Cambridge, United Kingdom). BD phosphoflow Perm Buffer III and Fix Buffer I were from BD Biosciences. RPMI 1640 GlutaMAX medium, fetal calf serum (FCS) and the barcoding fluorochromes Ax488 Succinimidyl Ester, Pacific Blue Succinimidyl Ester and Pacific Orange Succinimidyl Ester were from Thermo Fisher Scientific (Waltham, MA, USA).

Purification of B lymphocytes

B cells were purified from buffy coats by negative selection using RosetteSep Human B Cell Enrichment Cocktail (20 µl/ml blood) followed by Lymphoprep. CLL cells were isolated from whole blood by Lymphoprep according to manufacturer's protocol. Cell samples were cryopreserved in liquid nitrogen.

Phosphoflow experiments

The phosphoflow experiments were performed as described previously [23], with some modifications. See the following subsections.

Stimulation and fixation

B cells from healthy donors or CLL patients were incubated in RPMI 1640 GlutaMAX medium with 1% FCS and calibrated for 10 minutes in a 37°C water bath before pre-incubation as indicated with drugs or 0,001% DMSO as vehicle control, for 20 min. An unstimulated sample was taken before the cells were stimulated with anti-IgM (10 µg/ml) for the specified time periods. The harvested samples were fixed for 10 minutes in pre-warmed BD Phosphoflow™ Fix Buffer I at 37°C followed by two washes with PBS.

Fluorescent Cell Barcoding (FCB)

Fixed cells were resuspended in PBS and incubated with different concentrations of the barcoding fluorochromes Alexa Fluor 488, Pacific Orange and Pacific Blue (diluted in DMSO) in a 96-v-well plate. After staining in the dark for 20 min at room temperature, the cells were washed twice with flow wash (PBS, 10% FCS and 0.09% sodium azide), combined in one tube and permeabilized with BD Phosphoflow™ Perm Buffer III pre-stored at –20°C, and stored at –80°C.

Antibody staining and phosphoflow cytometry analysis

The permeabilized cells were washed three times with flow wash and spun for 5 min at 500g, resuspended and distributed into aliquots. The aliquots were stained with anti-CD19 surface marker conjugated with PerCP-Cy5.5 and, when indicated, with anti-CD5 conjugated to PE-Cy7, and the indicated phospho-specific antibodies

conjugated with Alexa Fluor 647, before they were incubated in the dark at room temperature for 30 min. Next, the samples were washed once, resuspended with flow wash and analyzed with a BD FACSCanto II (4-2-2) cytometer equipped with 405 nm, 488 nm and 633 nm lasers. Separately, unstimulated cells stained with Alexa Fluor 488, Pacific Orange and Pacific Blue, and compensation beads incubated with PerCP-Cy5.5- and Alexa Fluor 647-conjugated antibodies, were used for compensation. 150 000-500 000 events were recorded per sample (corresponding to 5 000-20 000 events per deconvoluted condition). Signals were calculated using the inverse hyperbolic sine (arcsinh) of the MFI (median fluorescent intensity) of phospho-signal versus isotype control, or of stimulated versus unstimulated cell populations, as described [24].

Analysis in Cytobank

The data were analyzed in Cytobank (https://cellmass.cytobank.org/cytobank/). By plotting SSC area versus FSC area, the lymphocytes were selected. Thereafter, single cells were selected by plotting FSC height versus FSC width. B cells were gated by plotting SSC area versus anti-CD19 PerCP-Cy5.5 and the FCB was selected by plotting Alexa Fluor 488, Pacific Blue and Pacific Orange against SSC area sequentially.

CellTiter-Glo luminescent cell viability assay and Dead Cell Apoptosis assay

CLL cells were co-cultured with CD40L+, BAFF+ and APRIL+ (ratio 1:1:1) L cells for 24 hours prior to initiation of the experiment to prevent induction of spontaneous apoptosis. The L cells were removed, and the CLL cells were incubated with the indicated drugs for 48 hours. CellTiter-Glo (Promega, Madison, WI, USA) reagent was subsequently added and luminescence was recorded after 10 min incubation at room temperature using an EnVision 2102 Multilabel Reader (PerkinElmer, Waltham, MA, USA). Alternatively, following drug incubation the cells were stained with FITC Annexin V and PI using a Dead Cell Apoptosis Kit from Thermo Fisher Scientific and analyzed with a BD FACSCanto II cytometer.

Statistical analysis

Statistical analyses were performed with R software (https://www.r-project.org) and Prism 7 (GraphPad Software, San Diego, CA). Analysis of the phosphorylation levels for 20 phospho-proteins was carried out via hypothesis testing in order to assess the significance of the differences between the CLL groups and the control, in particular between the means in the CLL groups and the value 1 (normalized to the control). The test used was an unpaired *t*-test for each phospho-protein sample.

The sample correlation between the different phosphorylation levels in the CLL group was calculated and tested for each phospho-protein pair. The statistical test used for this aim was the Pearson's product-moment correlation test (or Pearson's r-test), assessing if the correlation between two variables was significantly different from 0 (positive or negative). A p-value less than 0.05 was considered significant for this study.

The data were clustered via hierarchical agglomerative clustering. The dissimilarity between the phospho-protein CLL samples was assessed via standard Euclidean distance, while the linkage method used was Ward's method or average method.

Author contributions

IKM, JUH, LAM, KT and SSS designed the research. IKM, JUH and SSS performed the experiments and analyzed the data together with AC, LAM and KT. GET and LAM contributed material and interpreted data. IKM and SSS wrote the paper. All authors read and commented on draft versions of the manuscript and approved the final version.

ACKNOWLEDGMENTS

We thank Martine Schrøder, Marianne Enger, Jorun Solheim and Gladys Marie Tjørhom for expert technical assistance.

CONFLICTS OF INTEREST

The authors do not declare any conflicts of interest.

FUNDING

This work was supported by the Norwegian Cancer Society [grant numbers 5761237 and 419544], the Regional Health Authority for South-Eastern Norway [grant number 2015031], the Research Council of Norway [grant numbers 179573 and 187615] and the Stiftelsen Kristian Gerhard Jebsen.

REFERENCES

1. Teras LR, DeSantis CE, Cerhan JR, Morton LM, Jemal A, Flowers CR. 2016 US lymphoid malignancy statistics by World Health Organization subtypes. CA Cancer J Clin. 2016; 66:443–59.
2. Dal-Bo M, Bertoni F, Forconi F, Zucchetto A, Bomben R, Marasca R, Deaglio S, Laurenti L, Efremov DG, Gaidano G, Del Poeta G, Gattei V. Intrinsic and extrinsic factors influencing the clinical course of B-cell chronic lymphocytic

leukemia: prognostic markers with pathogenetic relevance. J Transl Med. 2009; 7:76.

3. Parikh SA, Shanafelt TD. Prognostic factors and risk stratification in chronic lymphocytic leukemia. Semin Oncol. 2016; 43:233–240.
4. Bertacchini J, Heidari N, Mediani L, Capitani S, Shahjahani M, Ahmadzadeh A, Saki N. Targeting PI3K/AKT/mTOR network for treatment of leukemia. Cell Mol Life Sci. 2015; 72:2337–2347.
5. Dighiero G, Hamblin TJ. Chronic lymphocytic leukaemia. Lancet. 2008; 371:1017–1029.
6. Zhong Y, Byrd JC, Dubovsky JA. The B-cell receptor pathway: a critical component of healthy and malignant immune biology. Semin Hematol. 2014; 51:206–218.
7. Burgler S, Gimeno A, Parente-Ribes A, Wang D, Os A, Devereux S, Jebsen P, Bogen B, Tjonnfjord GE, Munthe LA. Chronic lymphocytic leukemia cells express CD38 in response to Th1 cell-derived IFN-gamma by a T-bet-dependent mechanism. J Immunol. 2015; 194:827–835.
8. Rawlings JS, Rosler KM, Harrison DA. The JAK/STAT signaling pathway. J Cell Sci. 2004; 117:1281–1283.
9. Cramer P, Isfort S, Bahlo J, Stilgenbauer S, Dohner H, Bergmann M, Stauch M, Kneba M, Lange E, Langerbeins P, Pflug N, Kovacs G, Goede V, et al. Outcome of advanced chronic lymphocytic leukemia following different first-line and relapse therapies: a meta-analysis of five prospective trials by the German CLL Study Group (GCLLSG). Haematologica. 2015; 100:1451–1459.
10. Yu H, Pardoll D, Jove R. STATs in cancer inflammation and immunity: a leading role for STAT3. Nat Rev Cancer. 2009; 9:798–809.
11. Siveen KS, Sikka S, Surana R, Dai X, Zhang J, Kumar AP, Tan BK, Sethi G, Bishayee A. Targeting the STAT3 signaling pathway in cancer: role of synthetic and natural inhibitors. Biochim Biophys Acta. 2014; 1845:136–154.
12. Fabbri G, Dalla-Favera R. The molecular pathogenesis of chronic lymphocytic leukaemia. Nat Rev Cancer. 2016; 16:145–162.
13. Chiorazzi N, Ferrarini M. Cellular origin(s) of chronic lymphocytic leukemia: cautionary notes and additional considerations and possibilities. Blood. 2011; 117:1781–1791.
14. Bulgar AD, Snell M, Donze JR, Kirkland EB, Li L, Yang S, Xu Y, Gerson SL, Liu L. Targeting base excision repair suggests a new therapeutic strategy of fludarabine for the treatment of chronic lymphocytic leukemia. Leukemia. 2010; 24:1795–1799.
15. Rigoni M, Riganti C, Vitale C, Griggio V, Campia I, Robino M, Foglietta M, Castella B, Sciancalepore P, Buondonno I, Drandi D, Ladetto M, Boccadoro M, et al. Simvastatin and downstream inhibitors circumvent constitutive and stromal cell-induced resistance to doxorubicin in IGHV unmutated CLL cells. Oncotarget. 2015; 6:29833–29846. https://doi.org/10.18632/oncotarget.4006.
16. Srivastava RK, Srivastava AR, Korsmeyer SJ, Nesterova M, Cho-Chung YS, Longo DL. Involvement of microtubules in the regulation of Bcl2 phosphorylation and apoptosis through cyclic AMP-dependent protein kinase. Mol Cell Biol. 1998; 18:3509–3517.
17. Wang TH, Wang HS, Ichijo H, Giannakakou P, Foster JS, Fojo T, Wimalasena J. Microtubule-interfering agents activate c-Jun N-terminal kinase/stress-activated protein kinase through both Ras and apoptosis signal-regulating kinase pathways. J Biol Chem. 1998; 273:4928–4936.
18. Frank DA, Mahajan S, Ritz J. B lymphocytes from patients with chronic lymphocytic leukemia contain signal transducer and activator of transcription (STAT) 1 and STAT3 constitutively phosphorylated on serine residues. J Clin Invest. 1997; 100:3140–3148.
19. Myklebust JH, Brody J, Kohrt HE, Kolstad A, Czerwinski DK, Walchli S, Green MR, Troen G, Liestol K, Beiske K, Houot R, Delabie J, Alizadeh AA, et al. Distinct patterns of B-cell receptor signaling in non-Hodgkin lymphomas identified by single-cell profiling. Blood. 2017; 129:759–770.
20. Blix ES, Irish JM, Husebekk A, Delabie J, Forfang L, Tierens AM, Myklebust JH, Kolstad A. Phospho-specific flow cytometry identifies aberrant signaling in indolent B-cell lymphoma. BMC Cancer. 2012; 12:478.
21. Dores GM, Anderson WF, Curtis RE, Landgren O, Ostroumova E, Bluhm EC, Rabkin CS, Devesa SS, Linet MS. Chronic lymphocytic leukaemia and small lymphocytic lymphoma: overview of the descriptive epidemiology. Br J Haematol. 2007; 139:809–819.
22. Parente-Ribes A, Skånland SS, Burgler S, Os A, Wang D, Bogen B, Tjønnfjord GE, Tasken K, Munthe LA. Spleen tyrosine kinase inhibitors reduce CD40L-induced proliferation of chronic lymphocytic leukemia cells but not normal B cells. Haematologica. 2016; 101:e59-e62.
23. Skånland SS, Moltu K, Berge T, Aandahl EM, Tasken K. T-cell co-stimulation through the CD2 and CD28 co-receptors induces distinct signalling responses. Biochem J. 2014; 460:399–410.
24. Irish JM, Myklebust JH, Alizadeh AA, Houot R, Sharman JP, Czerwinski DK, Nolan GP, Levy R. B-cell signaling networks reveal a negative prognostic human lymphoma cell subset that emerges during tumor progression. Proc Natl Acad Sci USA. 2010; 107:12747–12754.